This document is confidential and is proprietary to the American Chemical Society and its authors. Do not copy or disclose without written permission. If you have received this item in error, notify the sender and delete all copies.

Structure, Dynamics, and Reactivity of Encapsulated Molecules in Restricted Spaces: Arylazoisoxazoles within an Octa Acid Capsule

Journal:	Langmuir	
Manuscript ID	la-2024-01996v.R2	
Manuscript Type:	Article	
Date Submitted by the Author:	n/a	
Complete List of Authors:	Sunny, Amal; University of Miami, Chemistry Cleven, Elliott; University of Miami, Chemistry Kumar, Pravesh; Indian Institute of Science, Education and Research Venkataramani, Sugumar; Indian Institute of Science, Education and Research, Walls, Jamie; University of Miami, Chemistry Ramamurthy, Vaidhyanathan; University of Miami, Chemistry;	

SCHOLARONE™ Manuscripts

Structure, Dynamics, and Reactivity of Encapsulated Molecules in Restricted Spaces: Arylazoisoxazoles within an Octa Acid Capsule

Amal Sam Sunny,^a Elliott C. Cleven,^a Pravesh Kumar,^b Sugumar Venkataramani,^b Jamie D. Walls ^{a,*} and Vaidhyanathan Ramamurthy ^{a,*}

^aDepartment of Chemistry, University of Miami, Coral Gables, FL 33146, USA
 ^bDepartment of Chemical Sciences, Indian Institute of Science Education and Research,
 Mohali, Sector 81, Knowledge City, Manauli – 140306, Punjab, India

Murthy1@miami.edu

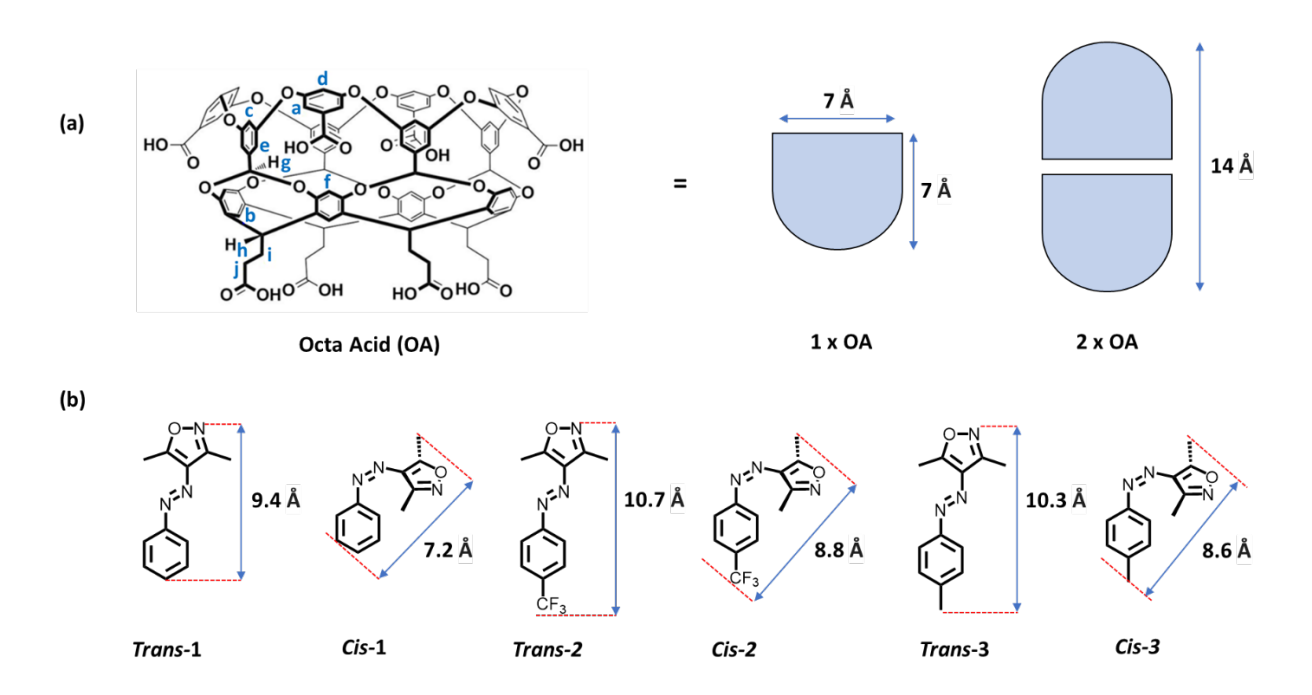
Abstract

In this study, a well-defined organic capsule assembled from two octa acid (OA) molecules acting as host and select arylazoisoxazoles (AAIO) acting as guests were employed to demonstrate that confined molecules have restricted freedom that translates into reaction selectivity in both ground and excited states. The behavior of these AAIO guests in confined capsules was found to be different from that found in both crystals, where there is very little freedom, and in isotropic solvents, where there is complete freedom. Through 1D and 2D ¹H NMR spectroscopic experiments, we have established a relationship between structure, dynamics and reactivity of molecules confined in an OA capsule. Introduction of CF₃ and CH₃ substitution at the 4-position of the aryl group of AAIO reveals that in addition to space confinement, weak interactions between the guest and the OA capsule control the dynamics and reactivity of guest molecules. ¹H NMR studies revealed that there is a temperaturedependence to guest molecules tumbling (180° rotation along the capsular short axis) within an OA capsule. While ¹H NMR points to the occurrence of tumbling motion, MD simulations and simulation of the temperature-dependent NMR signals provide an insight into the mechanism of tumbling within OA capsules. Thermal and photochemical isomerization of AAIO were found to occur within an OA capsule just as in organic solvents. The observed selectivity noted during thermal and photo induced isomerization of OA

encapsulated AAIOs can be qualitatively understood in terms of the well-known concepts due to Bell-Evans-Polanyi (BEP principle), Hammond and Zimmerman.

Introduction

Understanding and predicting the chemical behavior of molecules in ground and excited states require intimate knowledge of their nuclear and electronic structures and the dynamics of molecules in a given medium. Recognition that structure, dynamics, and reactivity are inter-related came into the forefront in the 60's under the name 'Hammond curriculum', which has revolutionized the way chemistry is taught and has led to tremendous growth in understanding the physical and chemical behavior of molecules in solution.¹⁻² The current study focusses on the reactivity of molecules in confined spaces that are only slightly larger than their molecular size.³⁻⁵ To understand the behavior of a confined molecule, it is important to determine both its molecular structure and dynamics in confined spaces as these are expected to be different than that found in free or unconfining isotropic solutions.⁶⁻⁷ The confined space that we are concerned with in this work is an organic capsule made up of two molecules of octa acid (OA; Scheme 1).8 The cavitand OA is known to form a capsular assembly in borate buffer in the presence of a guest molecule. The complex represented as guest@OA may have a guest to host ratio of 1:1 in a cavitandplex or either 1:2 or 2:2 in a capsuleplex. In this work, cis and trans arylazoisoxazoles 1-3 (Scheme 1) were chosen as guest molecules, 10 which was driven by the desire to probe the role of confinement on the geometric isomerization of N=N bonds in these molecules. 11-13 As a prelude to the studies on photochemical and thermal isomerization of 1-3, we have ascertained the structure and dynamics of 1-3 within an OA capsule in borate buffer using 1D and 2D NMR spectroscopy, ¹⁴ which are presented and discussed in the first and the second parts of this article.



Scheme 1: Chemical structure of (a) host octa acid (OA), and (b) guest molecules, along with their dimensions (including van der Waals radii).

One of our long-standing interests is to explore the role of 'free space' and 'weak interactions' on chemical reactions. 15-16 We have shown earlier that OA encapsulated molecules show selectivity and/or different reactivity from that found in isotropic solutions. 5, 17-19 In this context, we have chosen to explore the geometric isomerization of arylazoisoxazoles 2 and 3. The choice is dictated by the fact that CF₃ and CH₃ present at the 4-position of the aryl ring are nearly similar in size although their nature of their interaction with the aryl rings that comprise the OA interior is expected to be different. In the case of CH₃ the C—H---π interaction is stabilizing while in CF₃ the C—F---π interaction is destabilizing. 20 In prior studies we noticed that the isomerization of stilbenes (C=C) and azobenzenes (N=N) was prevented/slowed when the aryl rings were substituted with CH₃ groups at the 4-positions, which was attributed to C—H---π interactions. 5, 11-12, 21-24 In arylazoisoxazoles and related arylazo heterocyclic systems, theoretical calculations predict that *cis-trans* isomerization is favored through rotation/pyramidalization/hula twist of the aryl ring rather than the isoxazole ring. 25-32 Assuming the same mechanism holds within an OA

capsule, we envision that 2 and 3 provide an opportunity to probe the role of C—H--- π and C—F-- π interactions on isomerization pathways. Furthermore, unlike in stilbenes, *cis-trans* isomerization in azobenzene and related molecules can be triggered by both heat and light. This enables us to probe the role of confined spaces on the motion of molecules on both ground and excited state surfaces. Finally, it should be noted that during the last decade, there has been considerable interest in arylazoheterocycles in the context of their photochromic properties, most of it triggered by their applications. ^{25, 33-46} In solution, the isomerization of arylazoisoxazoles is known to be reversible and stable over many isomerization cycles. ^{10, 35-36, 38, 40-41} Establishing the reversibility within an OA capsule opens opportunities to exploit the photochromic properties of arylazoisoxazoles and possibly other azoheteroarenes for various applications in water. With these in mind and the knowledge gained from structure and dynamics mentioned above, we have examined the thermal and photochemical geometric isomerization of arylazoisoxazoles 2 and 3 included within an OA capsule. Since these molecules are not soluble in water, their behavior was compared with that observed in a DMSO solution. Results discussed here confirm that molecules confined in small spaces and dissolved in water are not rigid as they are in solids/crystals, and while their freedom is limited, it is not curtailed. This limited freedom leads to selectivity, which is the ultimate goal of organic chemists performing molecular transformations.

Experimental Section

Materials. Host Octa acid (OA) was synthesized and characterized according to the reported procedure. The guest molecules, *trans*-1, 2, and 3 were synthesized following the reported procedure. The *cis* isomers of the guest molecules were generated by exposing their respective *trans* isomers to UV light $(350 \pm 20 \text{ nm}, \text{ using a Luzchem reactor}, \text{ in either DMSO-d₆ or CD₃CN solvents), leading to the formation of approximately 98% of$ *cis* $isomer for all the three molecules (monitored by <math>^{1}\text{H NMR}$).

Instrumentation. All 1D NMR, 2D DOSY (Diffusion Ordered Spectroscopy), and 2D NOESY (Nuclear Overhauser Effect Spectroscopy) experiments were performed on either a 400 or 500 MHz NMR Bruker spectrometer. Chemical shifts are reported in parts per million (ppm). A deuterated solvent was used as a lock, and the residual protonated solvent peak was

used as a chemical shift reference. Absorption spectra were recorded on a Shimadzu UV - 3150 spectrophotometer.

General procedure for ¹H NMR titration experiments. A D₂O solution (600 μL) of OA (1 mM OA in 10 mM Na₂B₄O₇) was prepared in an NMR tube. To this solution, 0.25 equivalents of guest was added from its 60 mM stock solution in DMSO-d₆ or CD₃CN. The solution was then sonicated for 5 minutes, and the NMR spectra were recorded after each addition. Complexation was monitored by observing changes in the host and guest signals.

Procedure for NMR diffusion measurements. DOSY experiments were performed on Bruker 400 MHz NMR spectrometer. All the experiments were performed at 25 °C, at a host concentration of 1 mM (in buffered D₂O) and a guest concentration of 0.5 mM. Calculations and fittings of the diffusion data were done using TOPSPIN.

General procedure for competitive binding experiments. A 2:1 complex (host: guest) of OA and guest was prepared in buffered D_2O ([OA] = 1 mM and [guest] = 0.5 mM). To this solution, the competitive binding guest was gradually added from its stock solution. The solution was then sonicated for 5 minutes, and the NMR spectra were recorded after each addition. Complexation was monitored by observing the changes in the host and guest signals.

General procedure for variable temperature experiments. A 2:1 complex (host: guest) of OA and guest was prepared in buffered D_2O ([OA] = 1 mM and [guest] = 0.5 mM). 1H NMR spectra were recorded at various temperatures between 1 and 70 °C. The sample temperature was evaluated using a D_2O/TMS thermometer calibration curve for the spectrometer. 47

NMR simulation and determination of thermodynamic parameters. Variable temperature NMR spectra were fit with a simple model of exchange between two peaks using the MATLAB Curve Fitting Tool.⁴⁸ The exchange constant (k) was determined by these curve fits. Linearity of the resulting Eyring plots was shown to be most sensitive to the choice of transverse spin relaxation times (T2) at lower temperatures, causing large uncertainties in k. For this reason, initial guesses for relaxation constants were extrapolated from high temperature data. As suggested by Lente et. al, the extrapolation was done using both traditional Eyring plots (where the enthalpy of activation (ΔH^{\ddagger}) is determined by the slope and the entropy of activation (ΔS^{\ddagger}) by the y-intercept), as well as by modified Eyring

plots (where ΔH^{\ddagger} is determined by the y-intercept and ΔS^{\ddagger} by the slope) in order to increase the reliability of results.⁴⁹ This procedure was iterated until it converged.

General procedure for irradiation experiments. All samples were irradiated using a Luzchem reactor. For irradiation in the UV region, four blue lamps (350 ± 20 nm) were used, and for irradiation in the visible region, four white lamps (420 ± 20 nm) were used. For broadband irradiation, four blue lamps and four white lamps were used simultaneously. Irradiation was continued until there were no changes in the percent composition of the *cis* and *trans* isomers (percent composition monitored by 1 H NMR). The temperature inside the reactor was maintained below 35 $^{\circ}$ C at all times to minimize thermal reverse isomerization.

General procedure for thermal reverse isomerization (cis \rightarrow trans) experiments. The samples were irradiated with UV light to produce the corresponding cis isomers. These samples were then placed in a water bath with the required temperature (50, 60, 65, or 70 °C). The temperature was monitored by a thermometer. The samples were protected from light by wrapping them with aluminum foil. The ¹H NMR spectra were recorded at regular intervals.

Computational Methods: The MD simulations were performed using the following multi-step procedure.

Structures of host and guest molecules. The guest molecules, trans-1, 2, 3, cis-1, 2, and 3 were modeled using the Gauss View 5.0 program, and the 3D structure of OA was obtained from our previous study. These structures were then optimized at the B3LYP/GD3BJ level using the Gaussian 09 software package. In these calculations, O and N atoms were treated with the 6-31+g(d) basis set, and C and H atoms were treated with the 6-31g(d) basis set.

Charge calculation. The Restrained Electrostatic Potential (RESP) charges for OA and guest molecules were calculated and used to create topology files using Antechamber, an inbuilt tool in the AMBER program.⁵⁶

Starting structures of host-guest complexes. The initial structures of the host-guest complexes were obtained by performing a molecular docking procedure using the AutoDock Vina (version 1.5.6) program package.⁵⁷ The size of the grid was chosen to cover the host, and the spacing was kept to 1.00 Å. Each docking trial produced 20 poses with an exhaustiveness value equal to 20.

Molecular Dynamics (MD) simulations. The most promising poses obtained from the docking procedure were used for MD simulations using the GROMACS program package⁵⁸-⁵⁹ and AMBER03 force field. ⁶⁰ In all the simulations, the initial configuration, comprising the host-guest complex with sixteen negative charges (carboxylate anions), was positioned within a cubic box with dimensions $60\times60\times60$ Å³, and the residual volume of the enclosure was then populated with TIP3P water molecules.⁶¹ The system was then neutralized by replacing some water molecules with sodium and chloride ions. Energy minimization was then performed on these structures with the steepest descent method for 3000 steps. MD simulations were next performed on these energy-minimized structures for 200 ns using a constant number of particles (N), pressure (P), and temperature (T), i.e., an NPT ensemble. The bond lengths in OA were constrained by the LINCS algorithm⁶² whereas the SETTLE algorithm⁶³ was used to constrain the bond lengths and angles of the water molecules. A Particle-Mesh Ewald method⁶⁴ was used to calculate long-range electrostatic interactions. A time step of 2 fs was used to compute the MD trajectories for each model. The most representative structures for host–guest complexes were derived from a cluster analysis. While most simulations were run at 300 K, some were run at different temperatures (which are specified when required).

Binding energy calculation. The binding energy of guests within the host pocket was calculated using the Molecular Mechanics Poisson–Boltzmann Surface Area (MM-PBSA) method.⁶⁵

Analysis and visualization. Yasara,⁶⁶ Chimera,⁶⁷ and VMD⁶⁸ programs were used for visualization and preparation of structural diagrams.

Results and Discussion

Structure of arylazoisoxazole-OA complexes

Arylazoisoxazoles 1-3, which are insoluble in water, form clear solutions upon stirring with OA in a borate buffer due to the formation of host-guest complexes with OA. Indication of the inclusion of these molecules within OA comes from the corresponding ¹H NMR spectra shown in Figures 1 and 2. In Figures 1 and 2, the spectra of the pure OA in water (Fig 1a and Fig 2a) and D₂O solutions containing guests and host OA in the ratio of 1:2 (*cis* and *trans*-1-3, total of six, Fig. 1c, e, g and Fig 2c, e, g) and the guest alone in

DMSO-d₆ (Fig. 1b, d, f and Fig 2b, d, f) are provided. The most important indication that all six guest molecules were included within OA came from the upfield shift of the guest signals in the presence of OA.^{9, 69-70} For example, in *trans-1* and *trans-2*, the resonances for the two methyl groups on the isoxazole ring at $\delta \approx 2.5$ ppm in DMSO-d₆ were shifted to $\delta < 1$ ppm. Similarly in *cis* 1 and 2, the corresponding signals were shifted from $\delta \approx 2$ ppm to $\delta \approx 0$ ppm. Even larger shifts were observed for the 4-methyl group on the phenyl ring of *trans-3* ($\delta \approx 2.2$ ppm shifted to $\delta \leq -1$ ppm) and *cis-3* ($\delta \approx 2.5$ ppm shifted to $\delta \approx -1$ ppm). Such large upfield shifts have been previously attributed to the diamagnetic ring current of the aryl rings that form the capsule interior.^{9, 69-70} Further indication

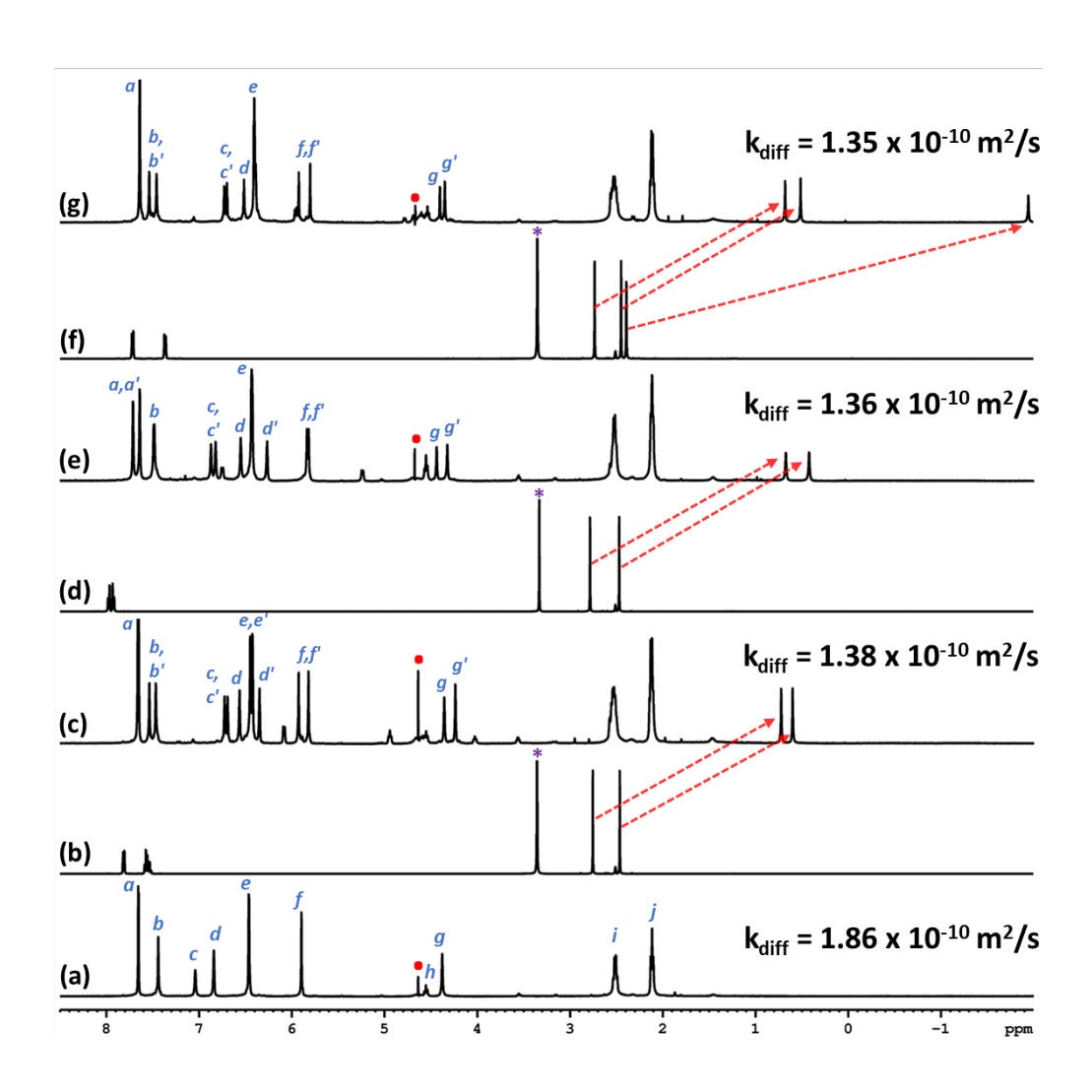


Figure 1: ¹H-NMR (500 MHz) spectra of (a) 1 mM OA, (b) *trans*-1, (c) *trans*-1@OA₂, (d) *trans*-2, (e) *trans*-2@OA₂, (f) *trans*-3, and (g) *trans*-3@OA₂. The NMR spectra of OA and host-guest complexes were recorded in buffered D₂O and that of free guests were recorded in DMSO-d₆. For all the host-guest complexes, [OA] = 1 mM and [guest] = 0.5 mM. The self-diffusion co-efficients are indicated with k_{diff} and red arrows denote the upfield shifted methyl signals of the guests upon complexation. The OA protons are labelled by *a-j* and the split OA signals upon complexation are labelled by *a*, *a*', *b*, *b*', etc. Ared dot represents residual D₂O, and * denote the HOD signal in DMSO-d₆.

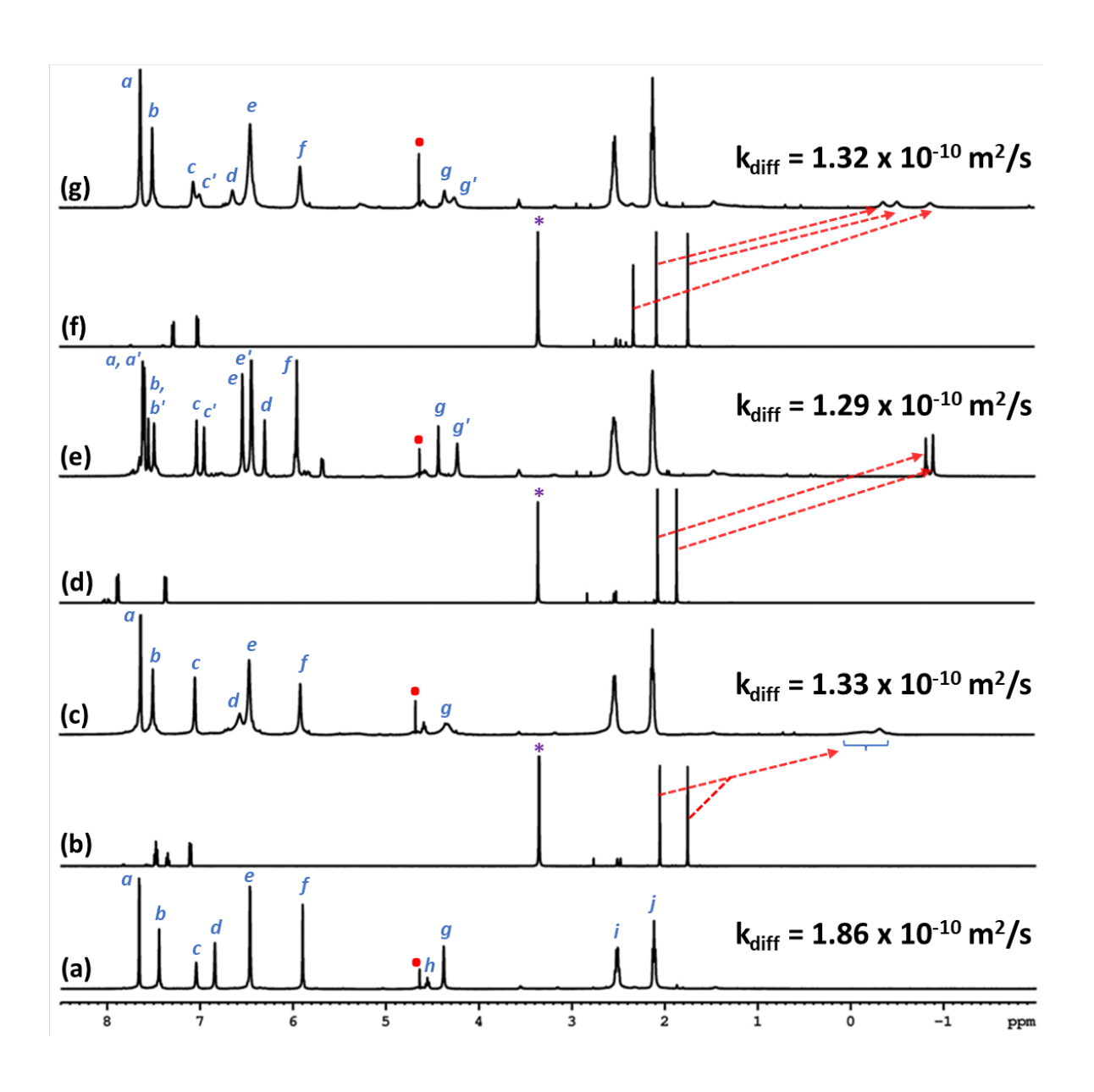


Figure 2: ¹H-NMR (500 MHz) spectra of (a) 1 mM OA, (b) *cis*-**1**, (c) *cis*-**1**@OA₂, (d) *cis*-**2**, (e) *cis*-**2**@OA₂, (f) *cis*-**3**, and (g) *cis*-**3**@OA₂. The NMR spectra of OA and host-guest complexes are recorded in buffered D₂O and that of free guests are recorded in DMSO-d₆. For all the host-guest complexes, [OA] = 1 mM and [guest] = 0.5 mM. The diffusion constants are indicated with k_{diff} and red arrows denote the upfield shifted methyl signals of the guests upon complexation. The OA protons are labelled by a-j and the split OA signals upon complexation are labelled by a, a, b, b, etc. Red dot represents residual D₂O, * denote the HOD signal in DMSO-d₆.

of the formation of complexes is observed from the change in the signals of the capsular hydrogens in OA. Comparison of the OA spectrum shown in Figures 1a and 2a with the complexed spectra reveals that signals from the OA hydrogens in the region 5.5 ppm $\leq \delta \leq 8$ ppm were disturbed (see Scheme 1 for OA peak assignments). Thus, the 1D ¹H NMR spectra unequivocally establish that guests **1-3** are included within OA. Further analysis of the spectra in Figures 1 and 2 reveal that the OA signals are split for the *cis-2* and **3** guests and for all three *trans* isomers with the methyl hydrogens of these guests appearing sharp whereas for the *cis-1* and **3** guests, the guest's methyl resonances were broadened. These observations are likely due to guest dynamics within the capsule, which will be discussed in the next section.

To determine the ratio of the number of guest to host molecules in each complex, we performed ^{1}H NMR titration studies by slowly adding concentrated DMSO solution of guest to an aqueous solution of OA in a borate buffer, an example of which is shown in Figure 3 for *trans-3* (similar spectra for other guests are provided in Figures S1-S3 in the Supporting Information section (SI)). In Figure 3, trace (a) provides the spectrum of OA with signal assignments as A, B, C etc. Upon the addition of *trans-3*, the disappearance of uncomplexed OA signals (A, B, C, etc.) was observed with the appearance of new signals for the complexed OA marked as, a, a', b, b', c, c' etc., and with observed upfield chemical shifts for the guest methyl signals in the range of -2 ppm $\leq \delta \leq 0$ ppm. It is important to note that some signals of complexed OA were split (*eg.*, b, b'; c, c', f, f' and g, g') upon inclusion of a guest

within OA as discussed above. The changes in the ¹H NMR spectra were gradual until the guest addition reached one half-equivalent of the host. At this stage no free OA was left in solution (trace (e)). This suggests that *trans-3* formed complex with OA in the ratio of 1:2. Similar conclusions can be reached for other guests by examining the spectra in Figures S1, S2 and S3 in SI. Further experimental evidence that 1:2 complexes were capsuleplexes also comes from the self-diffusion coefficients measured using a DOSY experiments (spectra provided in Figures S4-S9 in SI). While the self-diffusion coefficient for uncomplexed OA is 1.86x10⁻¹⁰ m²s⁻¹, the self-diffusion coefficients were around 1.30x10⁻¹⁰ m²s⁻¹ in the complexes, which was consistent with earlier studies that established self-diffusion coefficients close to 1.30x10⁻¹⁰ m²s⁻¹ and 1.55x10⁻¹⁰ m²s⁻¹ for OA capsuleplexes and OA cavitandplexes, respectively.^{69,71} Further confirmation of the G:H ratio was provided from the integration of the guest and host signals in the NMR spectra of the OA complexes (see Figures S10-S12 for details). Thus, from the NMR titration experiments, the observed self-diffusion coefficients, and the integration of the guest and host ¹H NMR signals, it appears that all six guest molecules form a closed capsule with OA in 1:2 (G:H) ratio.

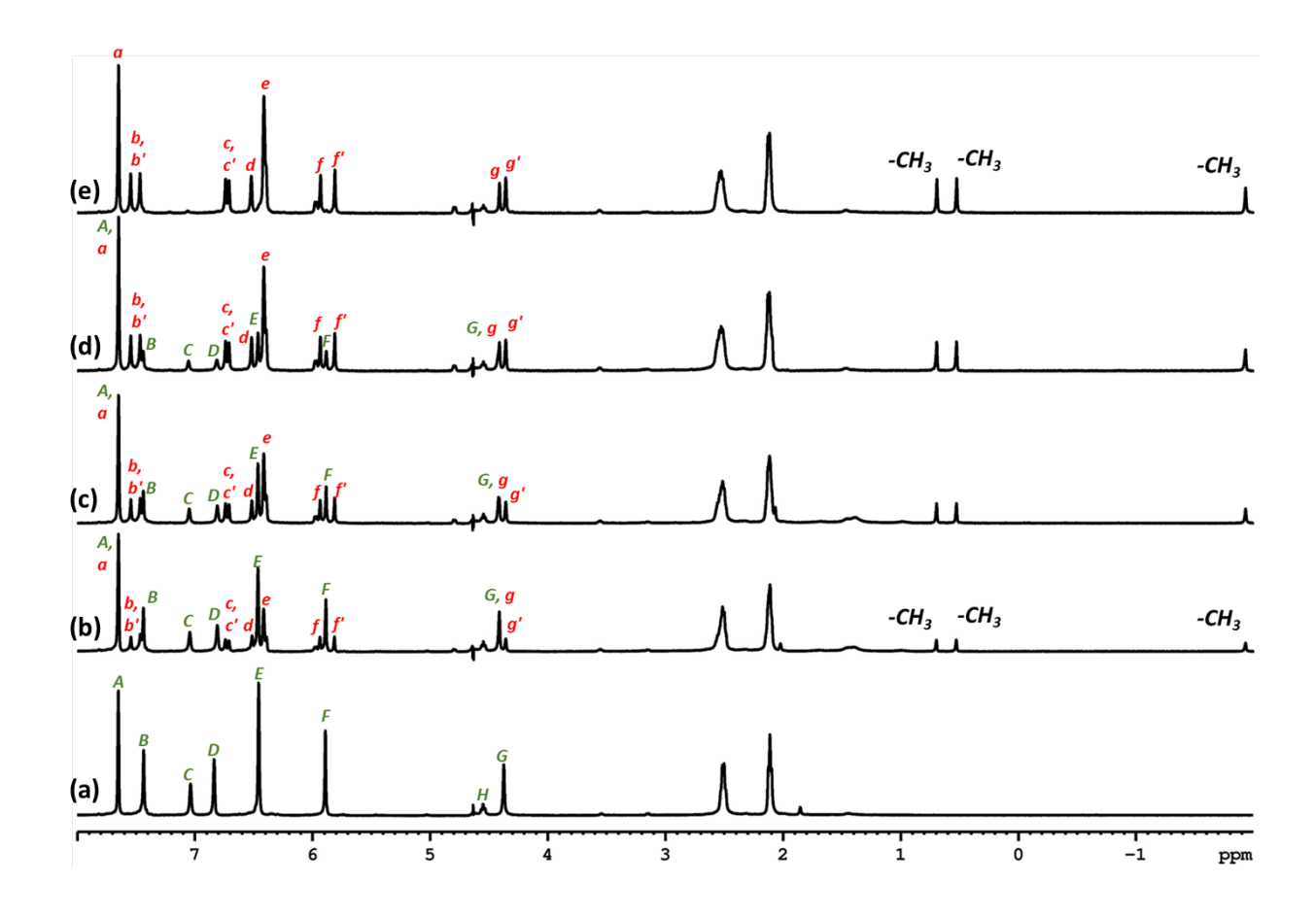


Figure 3: ¹H-NMR (500 MHz, buffered D₂O) spectra of titration of *trans*-3 with OA. (a) 1 mM OA, (b) 1 mM OA + 0.2 mM *trans*-3, (c) 1 mM OA + 0.3 mM *trans*-3, (d) 1 mM OA + 0.4 mM *trans*-3, and (e) 1 mM OA + 0.5 mM *trans*-3 The signals of free/uncomplexed OA are indicated by *A*-*G* and that of complexed OA are indicated by *a*, *b*, *b*, etc. Methyl signals of the complexed guest are indicated by –CH₃.

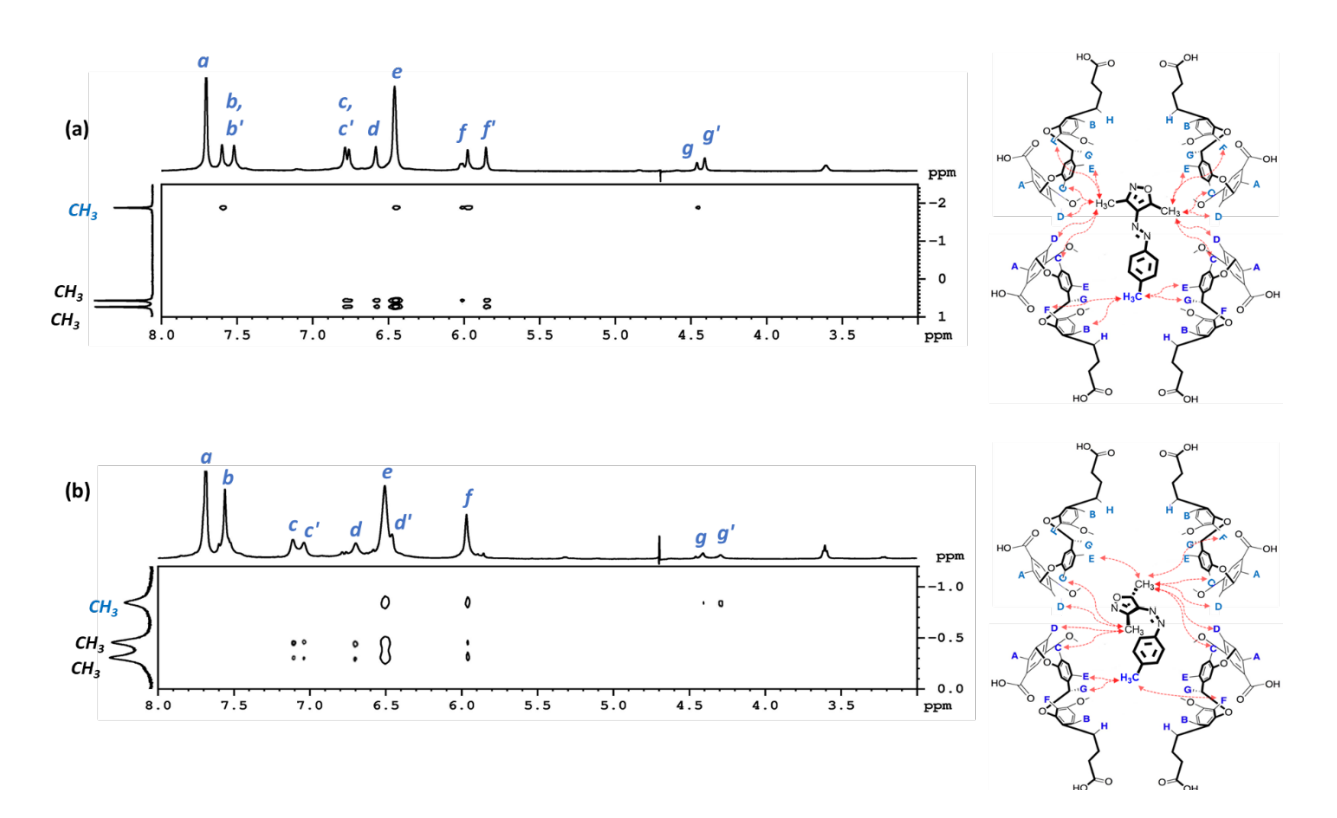


Figure 4: Partial 2D NOESY (500 MHz, buffered D_2O) spectra of (a) *trans*-3@OA₂, and (b) *cis*-3@OA₂. The structure of the host-guest complex is included. [OA] = 3 mM, [guest] = 1.5 mM.

To obtain additional insight into the structure of the guest molecule within an OA capsule, NOESY experiments (spectra provided in Figs. S13-S18 in SI) and MD simulations were carried out. The intermolecular proton correlations translated into pictorial representations are shown in Figure 4 for *trans*- and *cis*-3 guests (corresponding pictures for other guests are given in Figs. S13-S18 in SI). It should be noted that the signals from the two halves of the OA capsule have different chemical shifts due to the presence of the guest inside the capsule. From the NOESY analysis, the correlations of 4-methyl signals in *trans*- and *cis*-3 with the b, e, and f protons of OA (see Scheme 1 for assignments) suggest that this part of the molecule is buried deeper in the narrower part of the capsule. Similarly, the isoxazole methyl protons correlate with the d, e and f protons of OA suggesting that this part of the molecule is closer to the wider rim of the OA capsule. Given the length of the molecule, one would expect the phenyl to be in one half of the capsule with the isoxazole ring being in the other half. Similar analysis of the NOESY spectra given in SI reveals that

all guest molecules (*cis* and *trans* isomers) spread themselves between the two halves of the capsule. Since the guest molecules do not possess a horizonal plane of symmetry, the OA protons in the two halves should experience different chemical environments and hence be split. Thus, the observed splitting of the OA resonances in the capsuleplexes can be suggestive that a guest molecule is stationary (along the short axis of the capsule) within a capsule on the NMR time scale (in this case, defined by the inverse of the largest frequency difference between the corresponding resonances on different OA molecules making up the capsule). This will be discussed in more detail in the next section.

To complement the NOESY studies, MD simulations using the GROMACS program were carried out. The most representative structures and their binding energies (BE) calculated by the Molecular Mechanics Poisson-Boltzmann Surface Area method (MM-PBSA) for all six guest molecules are shown in Figures 5 and 6. These simulations confirm that the two parts of the guest are located within different halves of the capsule, with the azo chromophore that is involved in photochemical isomerization located predominantly within the middle wider region of the capsule. For the cis isomers that are shorter than the corresponding trans isomers, both the isoxazole and aryl rings were found to be closer to the middle region of the capsule. For cis-1 and cis-3 guests, the inter-cavitand distance between the two OA molecules forming the capsule was found to be a little larger than that found in capsuleplexes using the corresponding *trans* isomers (compare Figure 5 with Figure 6). Interestingly, in the case of guest 2, the inter-cavitand distance between OA molecules was nearly identical (within experimental error) for both the trans and cis isomers albeit a bit larger for the trans-2 isomer. On the basis of binding energies, one would expect the trans-1 and trans-3 guests to bind more strongly than the corresponding cis isomers (Figures 5 and 6). However, the binding energies of *trans* and *cis* isomers of 2 were similar within experimental error. Based on the above estimates of binding energies, one would expect the guests to bind with OA in the following order: $trans-3 > trans-1 > cis-2 \ge trans-2 > cis-3 > trans-2$ cis-1. In this series, as per the estimated binding energies, there is no preference between the cis-2 and trans-2 isomers for the OA interior within the error limits of the simulations.

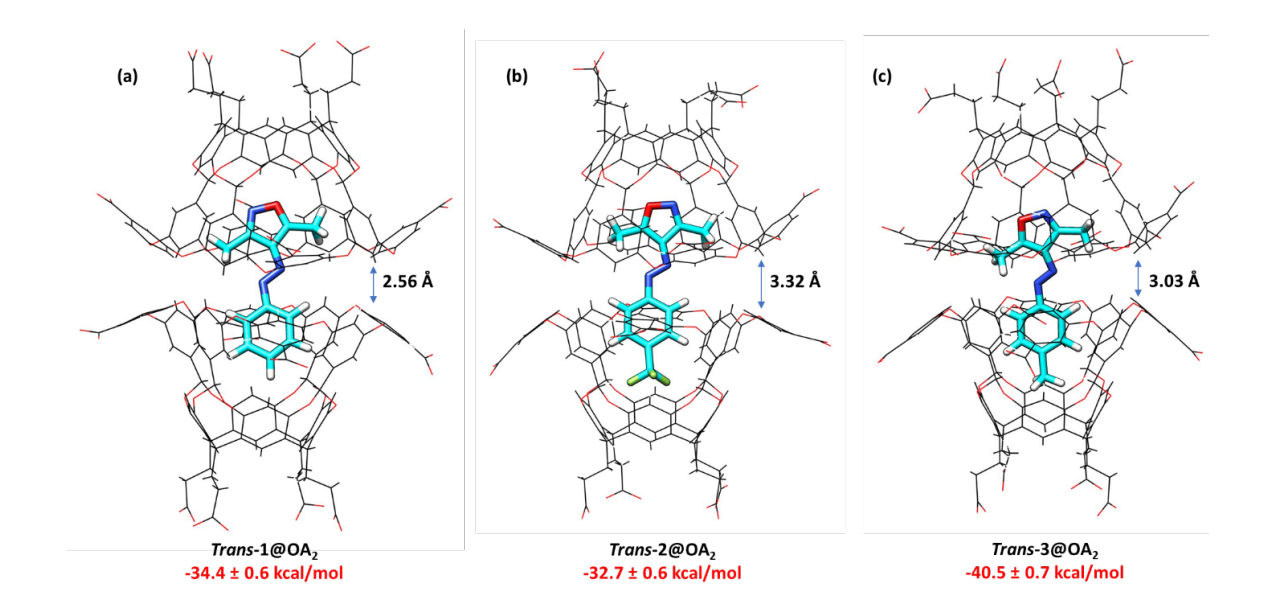


Figure 5: Structures of (a) *trans*-1@OA₂, (b) *trans*-2@OA₂, and (c) *trans*-3@OA₂ computationally generated by molecular dynamics simulations. The inter-cavitand distance and binding energy in each case is indicated. The simulations were performed for 200 ns, at 300 K.

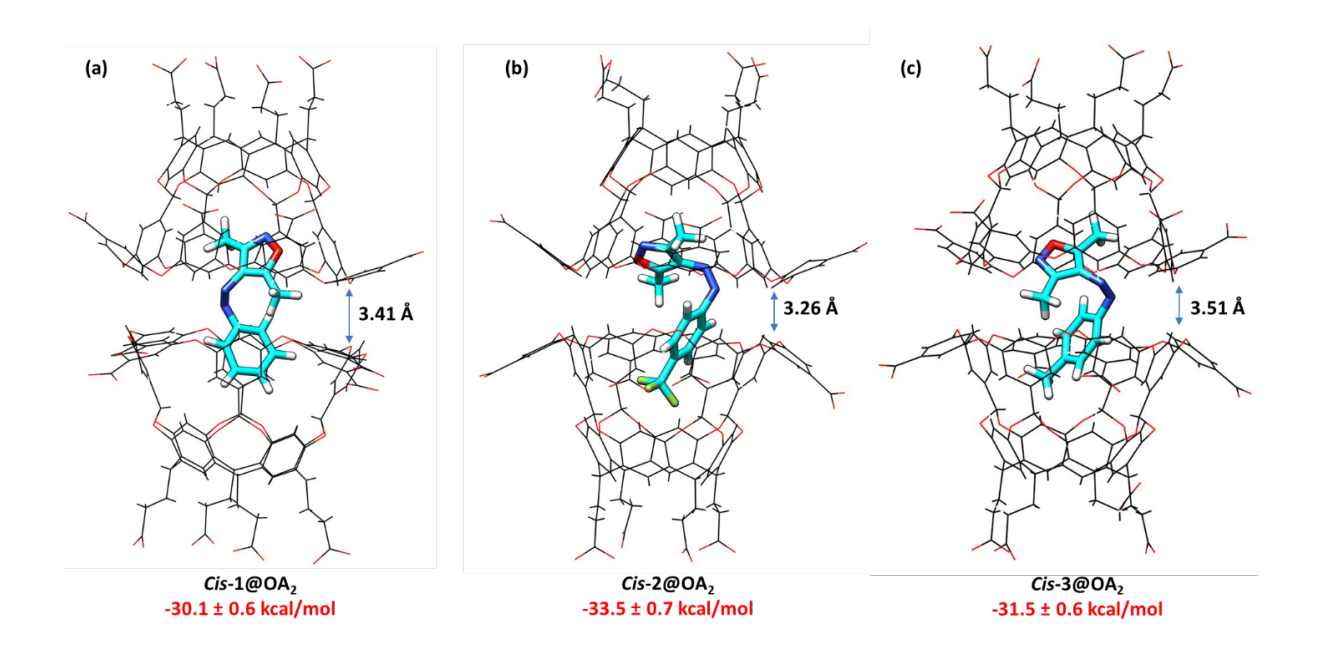


Figure 6: Structures of (a) *cis*-1@OA₂, (b) *cis*-2@OA₂, and (c) *cis*-3@OA₂ computationally generated by molecular dynamics simulations. The inter-cavitand distance and binding energy in each case is indicated. The simulations were performed for 200 ns, at 300 K.

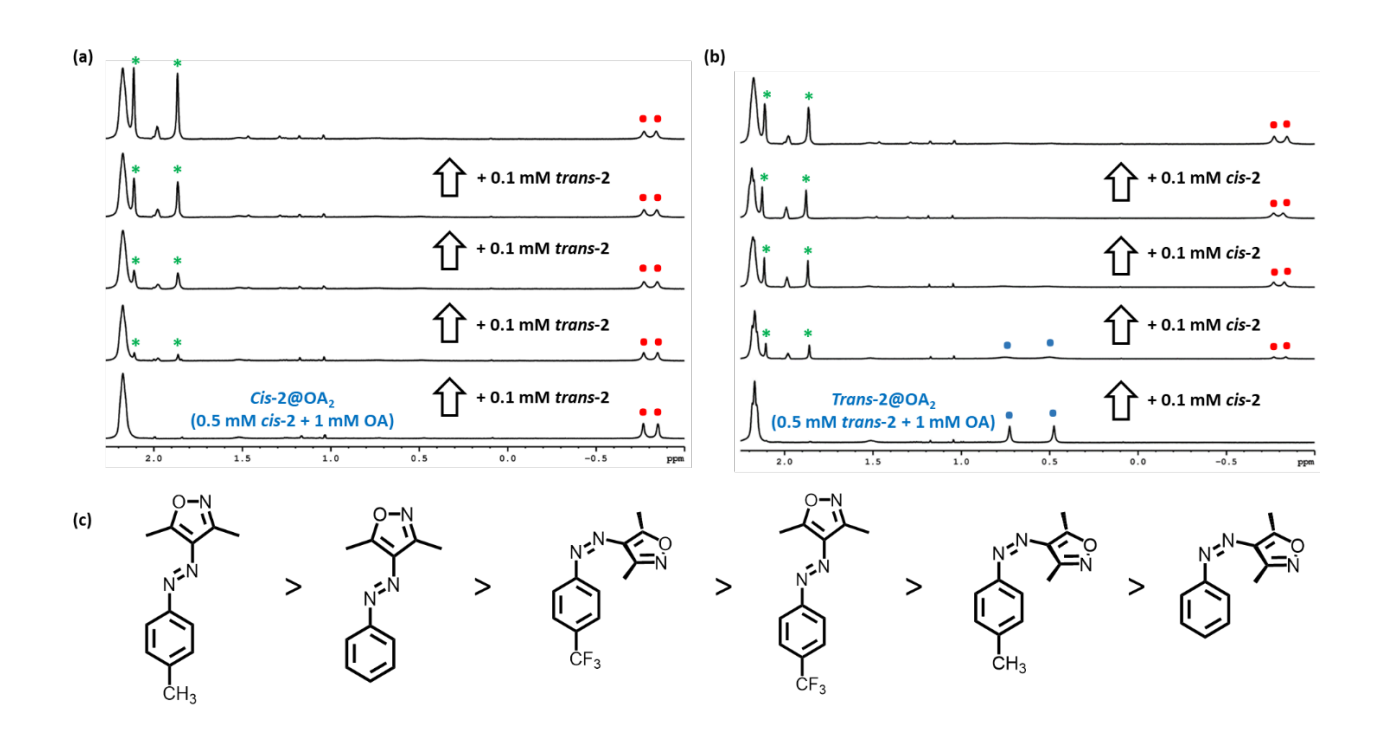


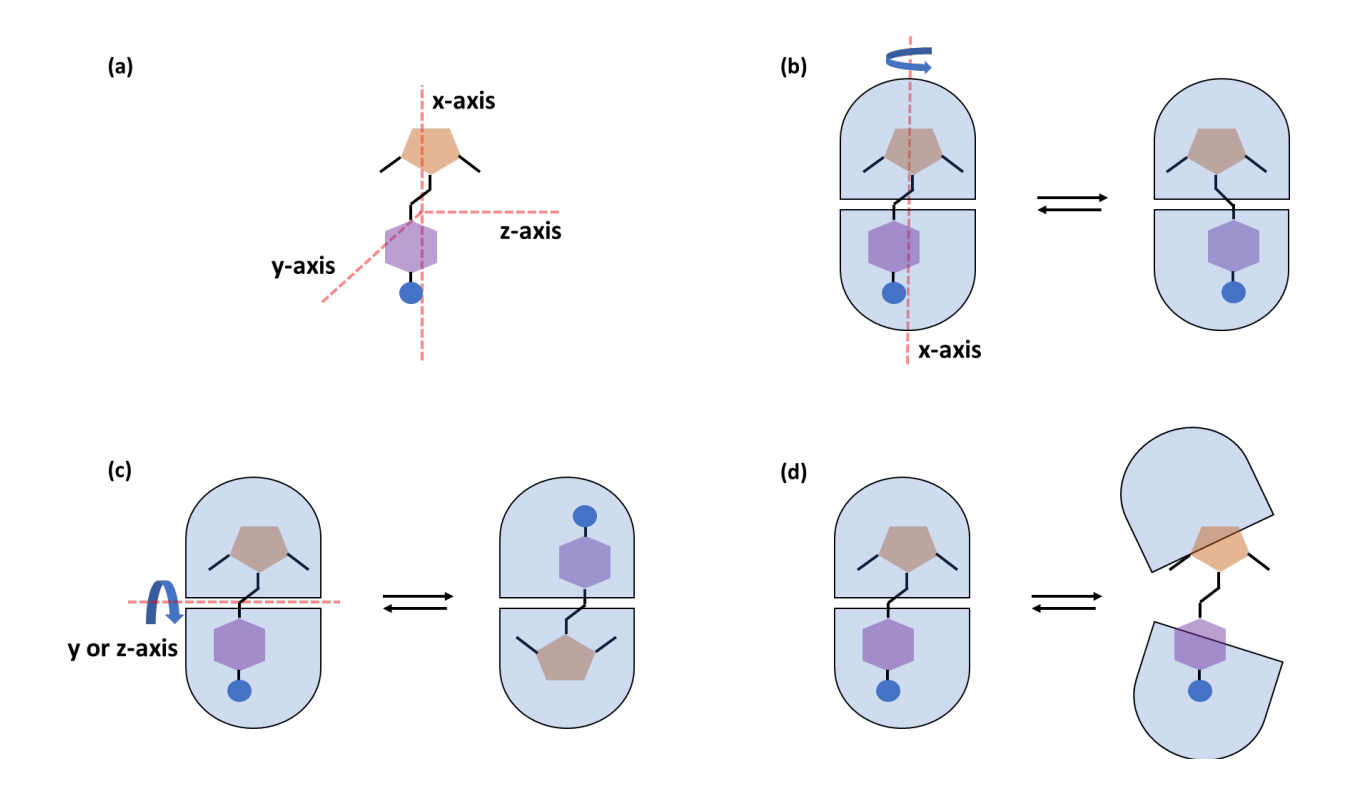
Figure 7: Partial ¹H-NMR (500 MHz, buffered D₂O) spectra of the competitive binding study between *trans*-2 and *cis*-2. (a) Addition of *trans*-2 to *cis*-2@OA₂ complex, and (b) addition of *cis*-2 to *trans*-2@OA₂. Red dots denote the methyl signals of complexed *cis*-2, blue dots denote the methyl signals of complexed *trans*-2, and green asterisks denote the methyl signals of uncomplexed *trans*-2 in water. (c) Trend of binding affinities of the guest molecules with OA obtained from competitive binding studies.

To verify the above computational predictions, competitive binding studies between the *cis* and *trans* isomers of **1-3** were carried out.⁷² This was performed by monitoring the changes in the ¹H NMR spectra when one guest was added to a solution of a different guest@OA₂. An example of such an experiment is presented in Figure 7 for the *cis* and *trans*

isomers of 2, which were predicted from the MD simulations to have similar binding energies. To examine whether *cis-2* could be displaced by *trans-2*, the latter was gradually added to a solution of cis-2@OA₂. As seen in Figure 7(a), upon addition of trans-2 there was no change in the signals due to cis-2@OA₂ at $\delta \approx$ -1 ppm. On the other hand, the added trans-2 signals were consistent with a trans-2 molecule in an aqueous environment (see signals at $\delta \approx 2$ ppm). This suggests that the *trans*-2 isomer is unable to displace the *cis*-2 isomer from an OA capsule. To further support this, the reverse experiment was also performed (Figure 7(b)) where the *cis* isomer was slowly added to a solution containing trans-2@OA₂. It was observed that upon addition of the cis-2 isomer, the signals due to cis-2@OA₂ start to appear while those for *trans*-2@OA₂ begin to diminish. During this process the trans-2 isomer is released into water. From the above competitive binding experiments it is clear that the cis-2 isomer forms a stronger complex than the corresponding trans-2 isomer; apparently, the binding energy difference of 1 kcal/mole between the isomers of 2 is real, and the competitive binding experiments were able to confirm this preference. Similar studies conducted on the other isomers (spectra given in S24-S32 in SI) revealed that the order of binding is trans-3 > trans-1 > cis-2 > trans-2 > cis-3 > cis-1, which is illustrated in Figure 7c.

Dynamics of arylazoisoxazole-OA complexes

Since the free space available for molecules within an OA capsule is much less than in a free, isotropic solution, the chemistry of OA confined guest molecules is expected to be different from that found in an isotropic solution. Knowledge of the dynamics of the guest molecules within the host is essential to predict the reaction pathways that a given confined molecule would be able to pursue. With this in mind, experiments focusing on the dynamics of *trans* and *cis* isomers of **1-3** within an OA capsule were performed. As illustrated in Scheme 2, guest molecules within an OA capsule may undergo at least two types of motions independent of the surrounding OA molecules, rotation along the long and short axes. In addition, the capsule itself could disassemble and assemble either partially or fully providing an encapsulated guest more space to tumble.^{69, 73-76}



Scheme 2: Cartoon representation of various motions of host – guest complexes. (a) Three axes of the guest, (b) rotation of guest about x (long) axis, (c) rotation of guest about y or z (short) axis, and (d) partial opening of OA capsule.

As demonstrated in the previous section, all guests form capsular assemblies, *i.e.*, the guest is held by two identical OA molecules. If the guest molecule was able to tumble freely within the capsule, one would expect the two OA molecules to have identical ¹H NMR chemical shifts. However, the majority of the ¹H spectra in Figures 1 and 2 reveal that several OA hydrogens, marked as a,a', b,b', c,c', d,d', e,e', f,f' and g.g', have different chemical shifts upon complexation with *trans-1-3*, and *cis-2* and 3. These signals are also in a 1:1 ratio, suggesting that the two OA molecules that comprise a capsule are no longer chemically identical.⁶⁹⁻⁷⁰ These observations also suggest that the tumbling motions of these guests are restricted within the capsule at room temperature. For the *cis-1* complex, however, the two OA molecules forming a capsule have identical chemical shifts (Figure 2c). This suggests that the *cis-1* isomer can tumble freely at room temperature within the capsule. To examine whether the tumbling could be arrested at lower temperatures, NMR spectra

down to 1°C were recorded for the *cis-***1** complex. The spectra, which are shown in Figure S38 in SI, reveal the *cis-***1** guest still freely tumbles within the OA capsule in the temperature range 1-50° C.

These observations suggest that for the OA encapsulated *trans*-1-3 and *cis*-2 and -3 guests to tumble freely inside an OA capsule, temperatures above room temperature are required. To probe this, 1 H NMR spectra of the complexes of the above guests were recorded at higher temperatures. One example illustrating the change in the 1 H NMR spectra with temperature is given in Figure 8 for *trans*-3@OA₂ (Figures S33-S37 in SI provide the spectra recorded for other guest molecules). As seen in Figure 8 and in Figures S33-S37 in SI, the split OA resonances coalesced with higher temperatures, suggesting that the tumbling of guests within the capsule is promoted upon thermal activation. The kinetic parameters involved in the tumbling process were estimated by fitting the variable temperature NMR spectra with a simple model of exchange between two peaks using the MATLAB Curve Fitting Tool (Figure 9).⁴⁸ The exchange constant (k) was determined by these curve fits. Eyring plots generated from these exchange constants gave ΔH^{\ddagger} and ΔS^{\ddagger} for the tumbling process of the guest within a complex, which are given in Table 1. An example of the curve fitting and Eyring plots for the (*trans*-3@OA₂) complex is given in Figure 9 (fits for the other molecules are given in Figs. S39-S43 in SI).

Since the 1 H NMR spectrum of cis-1 complexes was temperature independent, i.e., the molecule was freely tumbling over the experimental temperature range, ΔH^{\ddagger} and ΔS^{\ddagger} for the tumbling process could not be obtained. To gain an insight into the mechanism of cis-1@OA2 tumbling, MD simulations were performed, and the structures of the complex at various times (movie) were generated. Snapshots at five-time frames are shown in Figure 10. Clearly, this molecule flips within 45 ns without exiting the capsule. Apparently, slight opening of the capsule at 20 ns helps the molecule to reposition the phenyl and isoxazole groups from one part to the other part of the capsule within 45 ns. Most likely the initial larger opening of the complex (3.41 Å as illustrated in Figure 6), and the compact and shorter structure (length 7.2Å) enable cis-1 to tumble freely within the capsule without the capsule partially or fully disassembling. This is consistent with the 1 H NMR observations where the OA molecules within the capsule appear to be chemically equivalent.

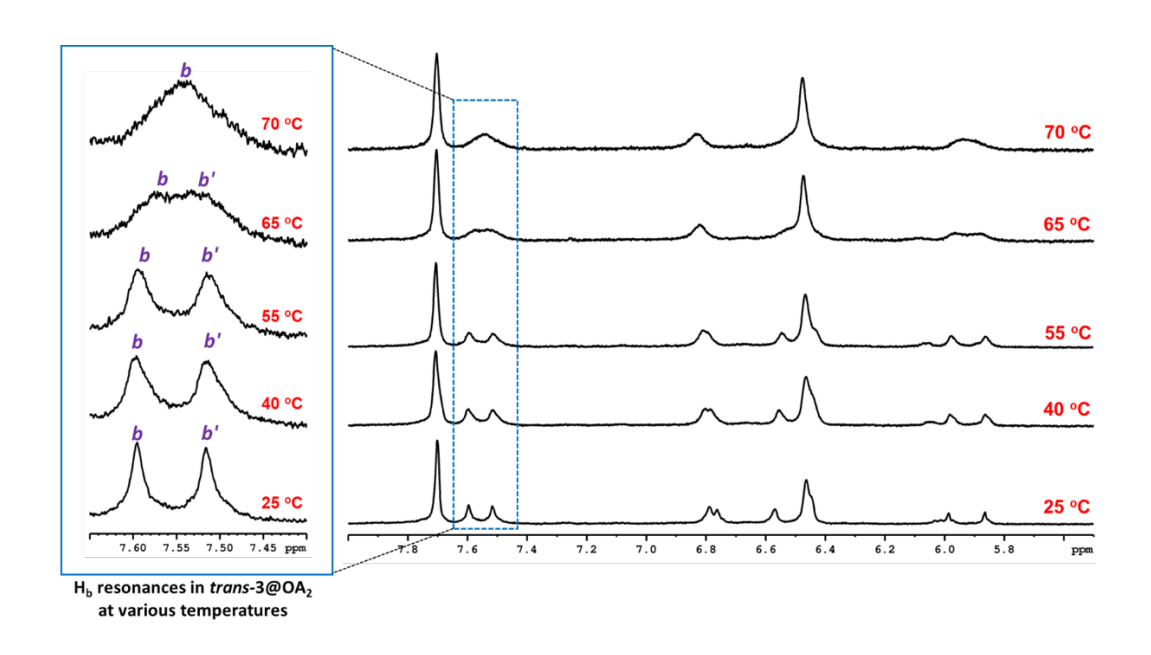


Figure 8: Partial ¹H-NMR (400 MHz, buffered D₂O) spectra of *trans*-3@OA₂ at various temperatures.

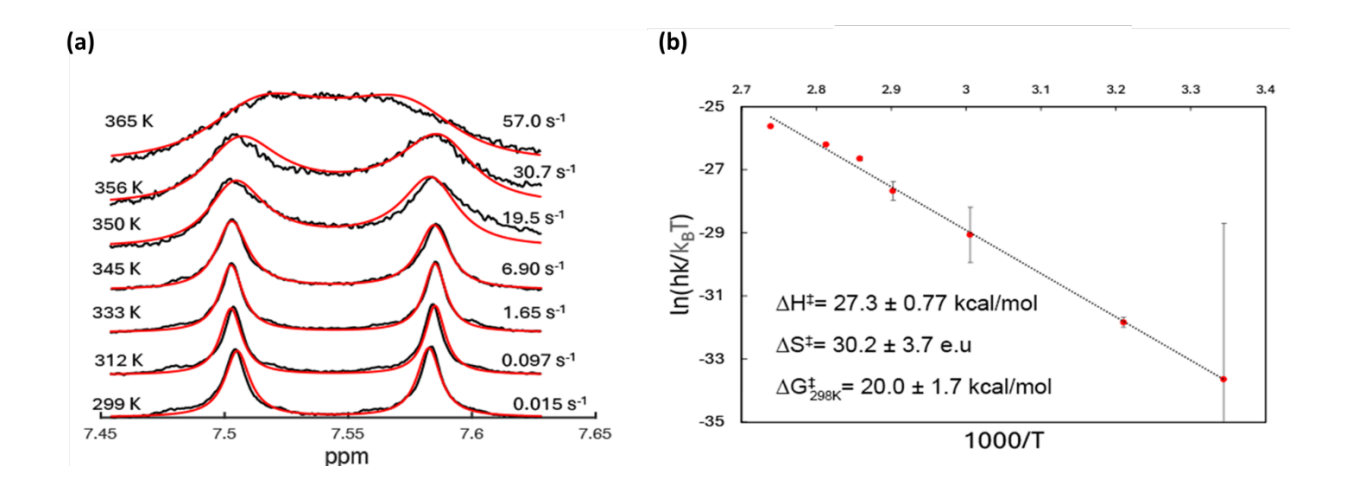


Figure 9: Determination of thermodynamic parameters for guest flipping within the OA capsule. (a) Partial ¹H-NMR spectra of *trans-3*@OA₂ complex at various temperatures (black) and the simulated spectra (red) along with the calculated rate constant of guest flipping at each temperature, (b) the Eyring plot generated from these rate constants along with the thermodynamic parameters.

Table 1: Activation parameters of guest@OA₂ complexes determined from simulations.^a

	ΔH [‡] (kcal/mol)	ΔS [‡] (e.u.)	ΔG [‡] _{25°C} (kcal/mol)
Trans- 1	27.2 ± 0.3	33.3 ± 1.0	19.2 ± 0.5
Trans- 2	22.0 ± 0.8	22.1 ± 3.2	16.8 ± 1.6
Trans- 3	27.3 ± 0.8	30.2 ± 3.7	20.0 ± 1.7
Cis-1	-	-	-
Cis -2	11.5 ± 0.8	-22.4 ± 3.2	16.9 ± 1.6
Cis- 3	17.6 ± 0.4	8.6 ± 1.8	15.6 ± 0.9

In *cis*-1@OA₂ the NMR signals are independent of temperature and are not split. Therefore, the thermodynamic parameters could not be estimated,

To gain an insight into the mechanism of tumbling of guest molecules that show temperature dependent NMR, we carried out similar MD simulations of OA complexes of these guests at 70 °C (Figure S20 and S22). Unlike *cis-*1, the *trans* 1-3 and *cis-*2 guests showed no indication of tumbling within 200 ns, although the capsules did expand in the middle likely giving more room for the guests to move. In the MD simulation at 70 °C, the

capsule came apart in the case of *cis-3* although the reason for this is not clear. Table S2 lists the inter-cavitand distance at both 27 °C and 70 °C. It was clear that in all cases, the two cavitands that make the capsule move apart slightly at 70 °C, which likely helps to facilitate the guest tumbling on a time scale longer than 200 ns. Consequence of this on thermal *cis-trans* isomerization is not obvious (see the later section). Because of the prohibitive computation cost involved, we did not go beyond 200 ns in our simulations.

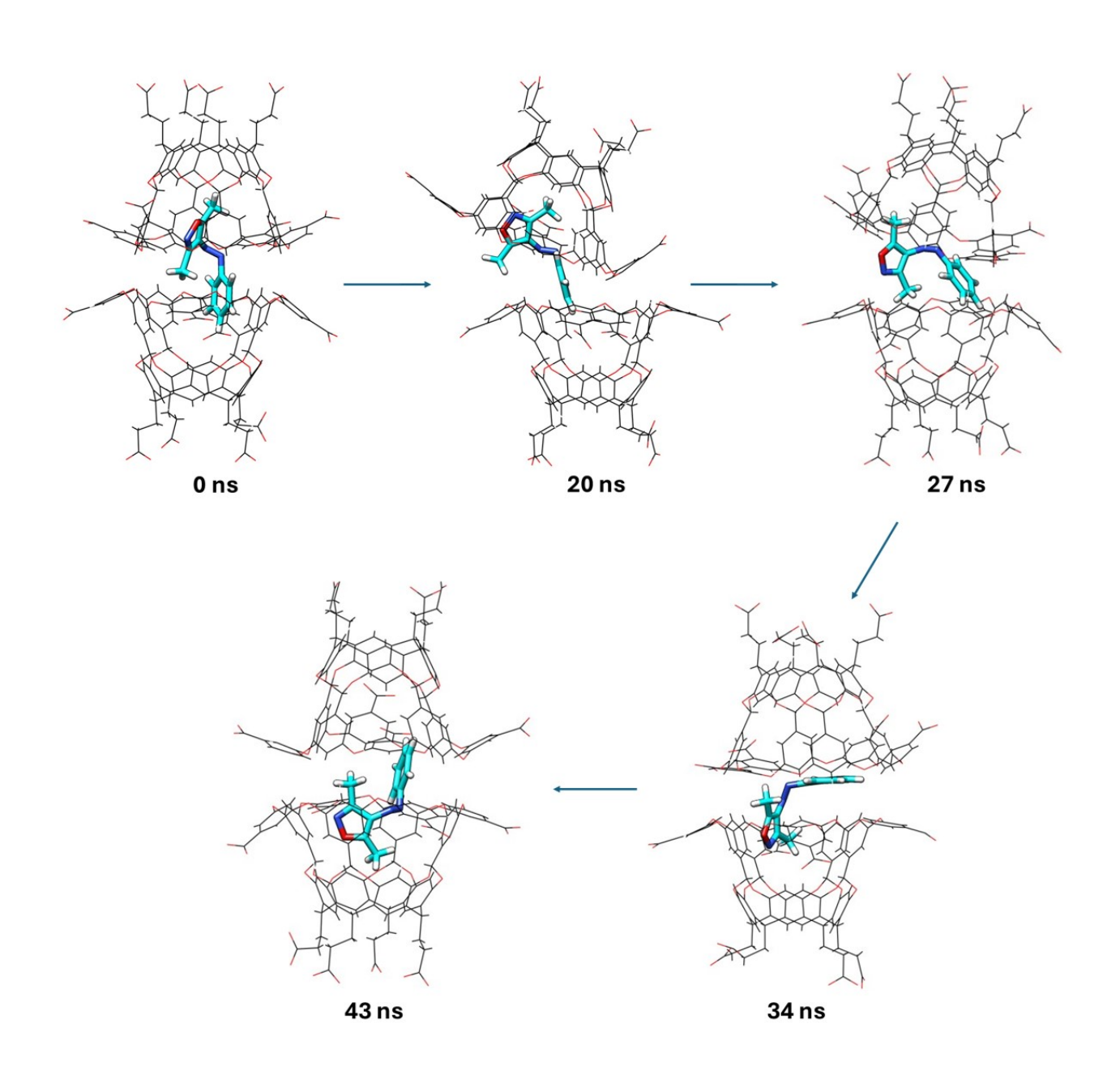


Figure 10: Snapshots of MD simulation of *cis*-1@OA₂ at different intervals. The simulation was done at 300 K.

Examination of Table 1 reveals the following trends: (a) In all cases, the process of tumbling involves positive ΔG^{\ddagger} and ΔH^{\ddagger} , (b) Tumbling results in positive ΔS^{\ddagger} in all cases except in *cis-2*, where ΔS^{\ddagger} is substantially negative. (c) Longer *trans* isomers have higher ΔH^{\ddagger} than the corresponding *cis* isomers (see Scheme 1 for lengths of guest molecules). (d) CF₃-substituted guests *trans-2* and *cis-2* have lower ΔH^{\ddagger} and ΔS^{\ddagger} than the corresponding hydrogenated *trans* and *cis-3* (compare CF₃ vs. CH₃). (e) Both *trans-3* and *cis-3* that are substituted with anchoring methyl groups have higher ΔH^{\ddagger} than the corresponding isomers of similar length and substituted with more hydrophobic CF₃ group. The latter, in fact, has no attractive interaction with the interior of the capsule whereas CH₃ does.^{20,77}

In analyzing the data in Table 1 it is important to note: (a) *trans* isomers are longer than the corresponding *cis* (Scheme 1). (b) The capsule is about ~7 Å in width (including van der Waals) at the wider region (wider entrance of the cavitand) and ~ 14 Å in length (Scheme 1). (c) Initial capsule opening at room temperature varies with the guest (Figures 5 and 6). (d) *Trans* isomers of 1 and 3 bind more strongly than the corresponding *cis* isomers (Figures 5 and 6). In the case of 2, the binding energies of the two isomers are almost similar although competitive binding studies showed that the *cis* binds more strongly.

Since the *trans* isomers are longer than the width of the capsule, these isomers will be unable to flip within a closed capsule. At the transition state of rotation, the guest molecule would have to partially free itself from the capsule and remain horizontal to the cavitand's median. This mechanism of tumbling is different from that of *cis-1* discussed above. In this process, a small part of the guest will be exposed to outside water molecules. Therefore, as the capsule expands/distorts to accommodate the rotation of the guest the freedom of water molecules closer to the mouth of the capsule would be affected. Thus, the measured positive ΔS^{\ddagger} is the result of freedom gained by the guest as well as surrounding water molecules. Interestingly, this model is able to rationalize even the small variations in ΔH^{\ddagger} and ΔS^{\ddagger} between the three *trans* isomers. For example, *trans-2* has lower ΔH^{\ddagger} and ΔS^{\ddagger} than *trans-3*. The only difference between the two is CF₃ vs CH₃. Larger ΔH^{\ddagger} for *trans-3* is likely due to

the weaker C–H--- π interaction between the CH₃ group and the four phenyl groups at the narrower end of the capsule. On the other hand, the CF₃ group has no specific interaction and in fact, there may be a repulsion between it and the four phenyl groups.²⁰ This is also reflected in the binding energies of the two guests estimated by MD simulations (Figure 5). Similarly, smaller positive ΔS^{\ddagger} for *trans-2* could be attributed to larger hydrophobicity of this group than CH₃. During the rotation, most likely the hydrophobic CF₃ group is exposed to surrounding water molecules prompting nearby water molecules more ordered and thus losing entropy. Such an effect is known earlier.

Interestingly cis-2 has negative ΔS^{\ddagger} whereas in the case of cis-3 it is positive. Straightforward rationale for negative ΔS^{\ddagger} is rotational motion occurring within the capsule like that in cis-1. We have reported negative ΔS^{\ddagger} for several aryl alkanes within OA capsule for similar tumbling motions. Since these are flexible molecules, we believed these molecules tumble within a capsule by exhibiting squiggly motions of methylene chains. Introduction of a C=C bond in the above aryl alkanes prevents such a motion. If this is the case, one would expect cis-2 and 3 with N=N bond would not be able to exhibit such squiggly motions. Most likely the tumbling of cis-2 and cis-3 occurs following the same mechanism as the trans isomers discussed above. If this is the case, the difference in ΔS^{\ddagger} could be due to the difference in hydrophobicity of 4-substituent (CF₃ vs CH₃) that would get exposed to surrounding water molecules.

From the above discussion it is clear that guest molecules within the capsule undergo tumbling motions that require 180° rotation or flip of the molecule within the capsule in order to make the ¹H-OA resonances appear to be equivalent. Also, the energy required for such a rotation depends on the substituent, with methyl groups apparently anchoring guest molecules better than CF₃ groups. We have explored these features in carrying out geometric isomerization of the above six azoisoxazoles encapsulated within OA capsules. Results are discussed in the next section.

Isomerization reactions of arylazoisoxazole-OA complexes

The above discussion reveals that the *capsule* is not a *casket*, *i.e.*, the content has flexibility. In the above section dynamics meant the reactant molecule was able to return to the original structure following some motions. In chemical reactions, which also involve

dynamics, the reactant molecule acquires a different structure (product) that may or may not fit well within the original space. In this section, we deal with a reaction known as geometric isomerization that transforms a linear *trans* isomer to a bent *cis isomer* and *vice-versa*. Arylazoisoxazoles **2** and **3** (Scheme 1) were chosen as probe molecules to examine whether the capsule would tolerate motions required for such a transformation. First, we examined thermal isomerization of *cis-***2** and *cis-***3** to the corresponding *trans* isomers. It is known that *cis-*azobenzenes thermally isomerize to *trans via* pyramidalization of one of the nitrogen centers in the N=N chromophore.^{13, 78} Prior studies on arylazoisoxazoles and related systems have established that the pyramidalization occurs at the aryl side rather than on the heterocyclic side.^{10, 25-26} This feature helps to probe the role of the 4-substituent (CF₃ and CH₃) on the isomerization process that involves a pyramidalization motion.

The *cis* isomers of **2** and **3** were prepared by irradiating the corresponding *trans* isomers with UV radiation (see below). As mentioned earlier (Figure 2), these form stable 1:2 complexes with OA. In solution, while the *trans* isomers are stable, the *cis* isomers thermally reverse to the trans at rates that are temperature dependent. The thermal isomerization of OA complexes of 2 and 3 were carried out at 50, 60, 65 and 70 °C by monitoring the reaction by ¹H NMR ((for results at 60°C, see Figures S44-S45 in SI). Arrhenius and Eyring plots presented in SI (Figures S50-S53) were linear. The energy of activation (E_a) obtained from Arrhenius plots for cis-2@OA₂ and cis-3@OA₂ in borate buffer were 40.4 ± 5.5 and 17.2 ± 2.2 kcal mol⁻¹. The free energies of activation (ΔG^{\ddagger}) estimated from Eyring plots, were 25.6 ± 7.4 and 22.5 ± 1.9 kcal mol⁻¹. Interestingly, the barrier for isomerization of cis-2 substituted with CF₃ is higher than that for cis-3 substituted with CH₃. In a DMSO solution, the barriers are nearly the same where energies of activation for cis-2 and cis-3 in DMSO are around 21 and 23 kcal mol⁻¹, respectively. Although the binding energies estimated from MD simulated structures of the trans isomers of 2 and 3 in an OA capsule are significantly different (-32.7 \pm 0.6 and -40.5 \pm 0.7 kcal mole⁻¹, respectively), the binding energies for the corresponding cis-isomers in an OA capsule are similar (-33.5 \pm 0.7 and -31.5 ± 0.6 kcal mole⁻¹, respectively (Figures 5 and 6)). The lower barrier for thermal isomerization of cis-3 to trans-3 with respect to cis-2 to trans-2 within an OA capsule is likely to be due to better binding of the product, in this case, trans-3 relative to trans-2. This is in accordance with the well-known Bell-Evans-Polanyi principle, which connects the ΔG

to ΔG^{\ddagger} of a reaction.⁷⁹ Since the free space inside the capsule for both *cis-2* and *cis-3* is expected to be nearly the same (342.63 Å³ and 347.59 Å³ respectively), the lower activation energy for *cis* to *trans 3* is likely to be the result of the product binding better than the reactant to the OA interior through C—H--- π interaction (Figure 11a) Thus, by comparing the behavior of *cis-3*@OA₂ and *cis-2*@OA₂ we are able to demonstrate the role of weak interaction in driving reactions within a capsule.

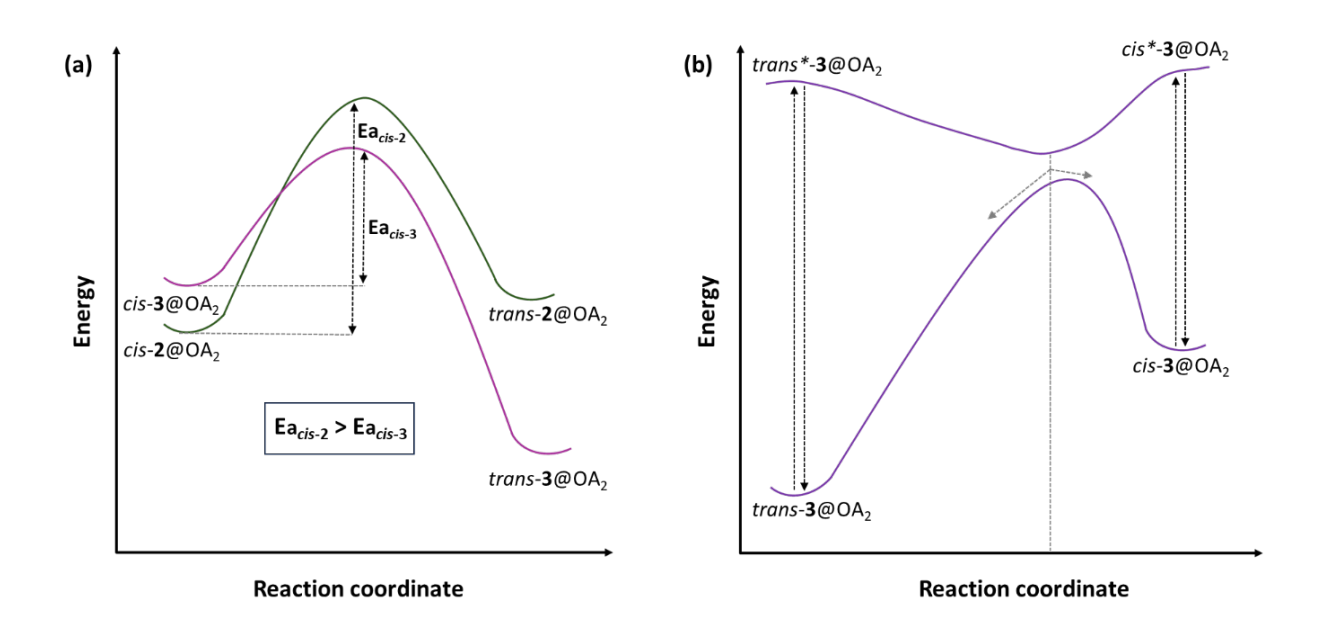


Figure 11: (a) Potential energy diagrams for thermal Z-E isomerization (the barriers are estimated based on the Eyring/Arrhenius plots) (b) schematic representation of photoisomerization involving avoided crossing.

Unlike thermal isomerization of *cis* to *trans*, photochemical isomerization is more complex. Even for azobenzene, several mechanisms and reactions from both lower and upper excited states have been proposed. 11-13, 23, 27, 29, 32, 78, 80-85 Several ultrafast experiments and quantum chemical calculations have been carried out without any final word on the mechanism. 5, 11-12, 23, 32, 81-82 Within an OA capsule as we have demonstrated, new pathways that are absent become available. Thus, the mechanism of photoinduced geometric isomerization of OA encapsulated arylazoisoxazoles is expected to be more complicated than

for thermal processes. To the best of our knowledge, there are only very few ultrafast time resolved study on azoheteroarene, but none on arvlazoisoxazoles.^{30, 86} These studies propose that the isomerization of the N=N bond occurs via a hula-twist of the phenyl part of the molecule. 87-92 Due to lack of further knowledge, we assume the same mechanism also holds during the photoisomerization of arylazoisoxazoles in solution and within an OA capsule. Whatever the mechanism, the aryl group needs to be displaced from the original site within capsule. This process would be influenced by the group present at the 4- position of the aryl ring. Our goal is to establish the role of capsule-reactant weak interaction on isomerization using 2 and 3 as probes. Independent of the mechanism of cis-trans isomerization, namely torsional rotation, pyramidalization, a combination of the two, or a hula-twist (Figure 12), the photostationary state composition at a given wavelength of irradiation would depend on the geometry at which the excited and ground state surfaces become closest in energy, i.e., near a conical intersection. We believe that the nature of the ground state surface that we utilized to understand thermal reaction would play a role during the excited molecule's entry from excited to ground state surface. What process brings the excited molecule to the CI is not obvious. At this stage, we do not have any evidence in favor of one process over the other (Figure 12). Given the current surge in evidence in favor of hula-twist mechanism during cis-trans isomerization, this process can't be ignored in arylazoisoxazoles. 81, 86, 88, 90-91, 93-94 Especially within the confined space of the OA capsule volume conserving hula-twist mechanism is likely. We are aware that only ultrafast time resolved experiments and highlevel computations can provide an in-depth and unequivocal understanding of the photoisomerization process in solution and within an OA capsule. We hope to pursue such studies in the future.

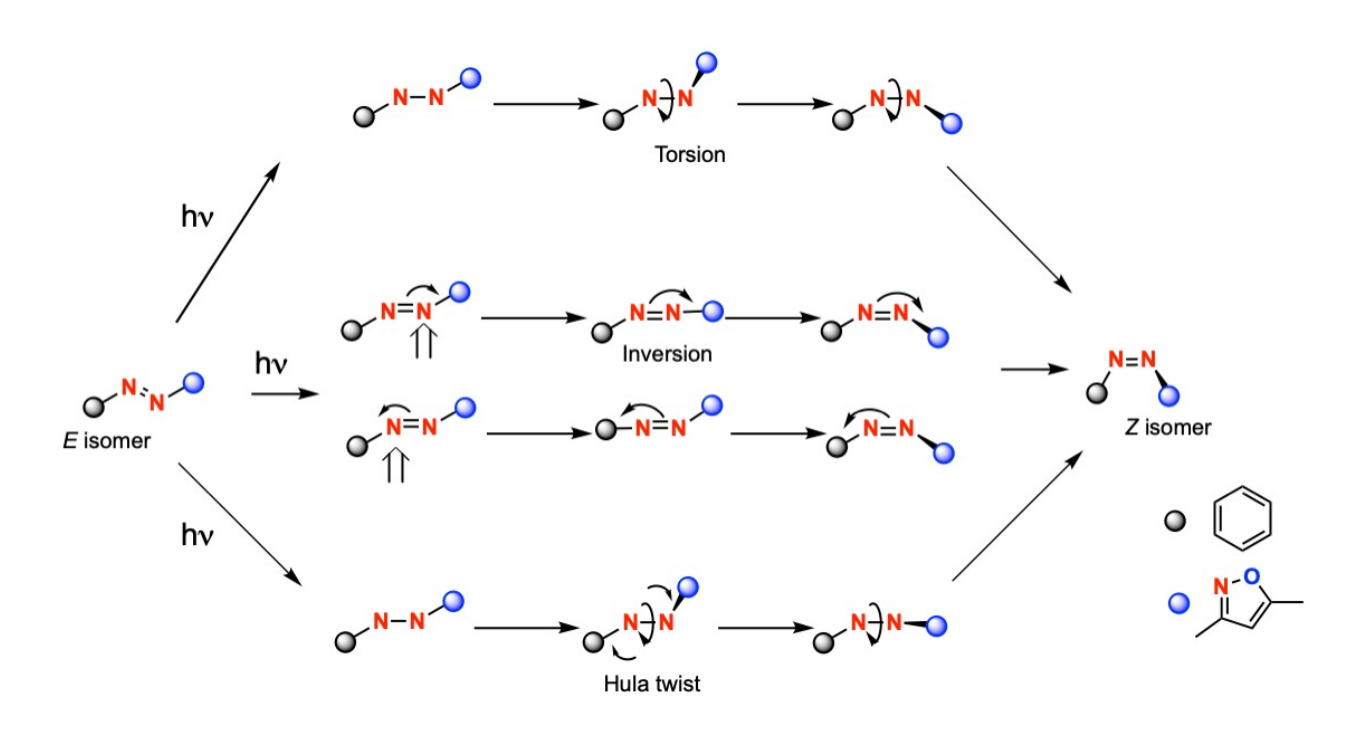


Figure 12. Schematic illustration of possible three modes of photochemical cis-trans isomerization of arylazoisoxazoles.

In Figure 13, the absorption spectra of *trans* and *cis*-2 and 3 in DMSO and encapsulated in OA are provided. As expected, there are two distinct non-overlapping absorptions due to $n\pi^*$ and $\pi\pi^*$ transitions. The large separation between S_1 and S_2 (~15 kcal mole⁻¹) is the ideal condition for violation of Kasha's rule i.e., reactions from upper state S_2 . In the current study, excitation with three different regions of light were conducted, (a) visible light (420±20 nm), (b) UV light (350±20 nm) and (c) light of $\lambda > 320$ nm. To test the reversibility of the isomerization, i.e., its photochromic nature, UV and visible excitations were done in sequence. Figures 13 and 14 provide the ¹H NMR spectra of such irradiations of *trans*-2@OA₂ and *trans*-3@OA₂. UV irradiation of *trans*-2@OA₂ resulted in 99% *cis*-2@OA₂ while irradiation of *trans*-3@OA₂ gave 89% *cis*-3@OA₂. Since longer irradiation did not alter the *cis*-*trans* composition, we used this composition to examine the photochemistry of the *cis* isomers upon excitation to S_1 . The photostationary state upon visible irradiation of *cis*-2 and *cis*-3 in DMSO was found to consist of 75% *trans* and 25% *cis*, identical for both guests. On the other hand, in the case of *cis*-2@OA₂ and *cis*-3@OA₂ the photostationary

states were found to contain 74% and 100% trans respectively. Obviously, OA capsule favors the trans when the 4-substituent in the aryl group is CH₃. We believe the excited molecule in the S₁ surface, independent of the path it takes (torsional, pyramidalization, a combination of the two, or a hula-twist) would enter the ground state surface near 90° twisted geometry. At this entry point, if the ground state surface is not symmetrical, the cis and trans isomers would be expected to be formed in unequal amounts. If the transition state in the ground state surface is closer to the cis, the entry from S₁ to S₀ would favor the trans isomer (Figure 11b). Since the difference in binding energies between the *cis* and *trans* isomers is larger in trans-3@OA₂ than in trans-2@OA₂ (Figures 5 and 6), we hypothesize that the entry point (conical intersection) would favor the *trans* isomer in *trans*-3@OA₂. This qualitative interpretation of results is based on Zimmermann's original proposal⁹⁵ that the entry of molecules from the excited state surface to the ground state surface would occur near the maximum on the ground state surface, and Hammond's postulate⁹⁶ that the maximum on the ground state surface (transition state) connecting the reactant and product would be closer to the structure with higher energy. This simple model based on well-established concepts explains the observed difference in photostationary state composition between 2 and 3. We are aware that the reaction co-ordinates for the ground and excited reactions don't have to be the same but that would not affect the energy difference in the ground state. Further the conical intersection (CI) through which the excited molecule enters the ground surface could be a different point than the one shown in Figure 11(b). In modern times when CI plays an important role, the model proposed here may be too primitive. 97-99 Yet, it is interesting to note that the observed results could be rationalized based on well-established early concepts more familiar to organic chemists. We plan to pursue quantum chemical calculations to fully comprehend the mechanism of geometric isomerization in a confined space.

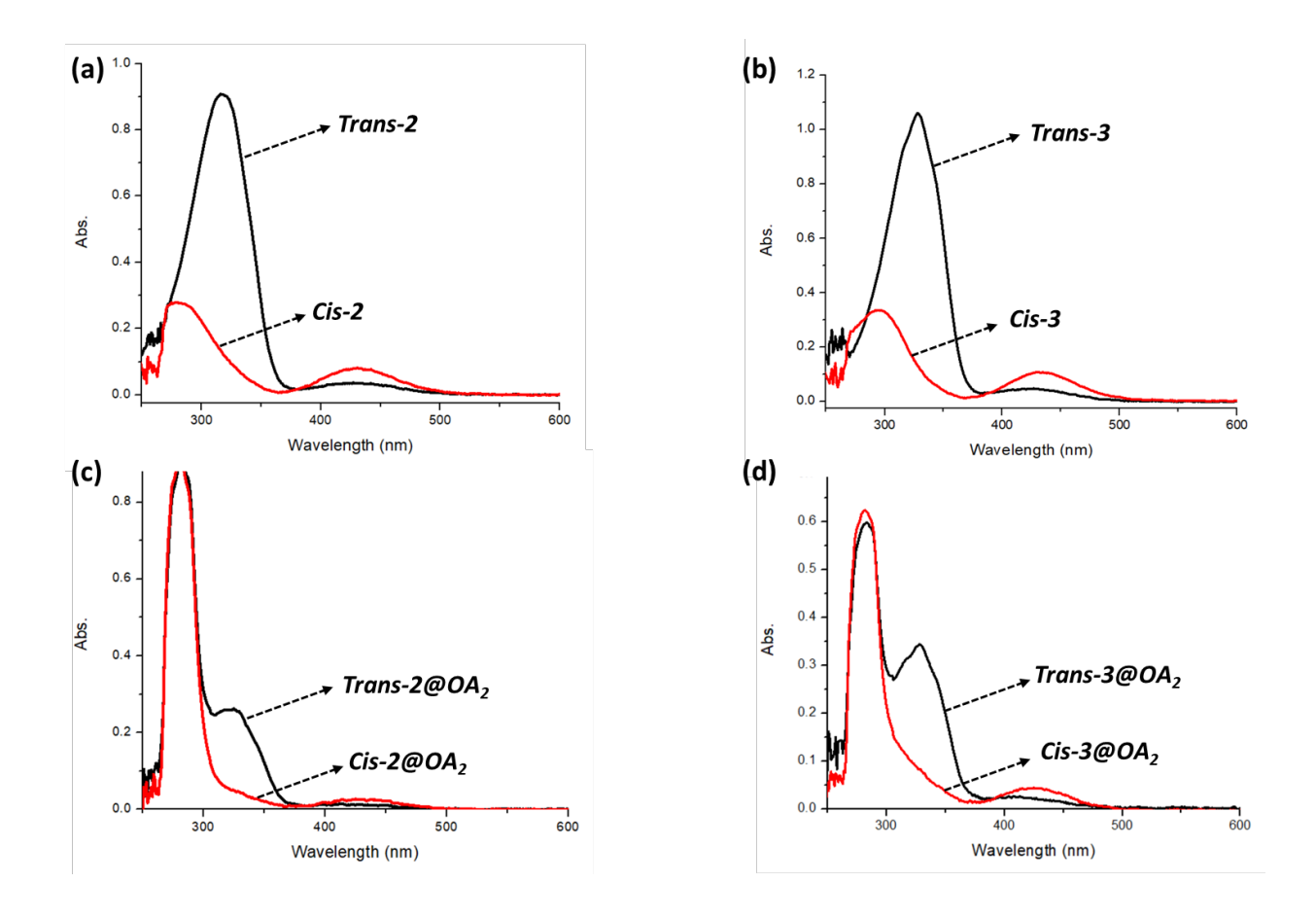


Figure 13: Absorption spectra of (a) *trans* and *cis-***2** in DMSO, (b) *trans* and *cis-***3** in DMSO, (c) *trans-***2**@OA₂ and *cis-***2**@OA₂ in borate buffer, and (d) *trans-***3**@OA₂ and *cis-***3**@OA₂ in borate buffer. ([OA] = $4 \times 10^{-5} \text{ M}$, [guest] in OA complexes is $2 \times 10^{-5} \text{ M}$, and in solution, DMSO, is $5 \times 10^{-5} \text{ M}$)

To confirm the role of CF₃ and CH₃ on the isomerization, we carried out broad band irradiation (320-500 nm) of all four molecules in both OA capsules in D₂O, cis-2@OA₂, cis-3@OA₂, trans-2@OA₂ and trans-3@OA₂, and in DMSO. The photostationary state in DMSO were 40:60 and 47:53 (cis:trans) for 2 and 3 while those found in OA complexes were 51:49 and 12:88 for 2@OA₂ and 3@OA₂, respectively. Clearly the trans isomer is favored in the case of 3. The photostationary state depends on the absorption ratio multiplied by the decay ratio (see SI for details). Knowing the absorption efficiencies of the two isomers at various wavelengths, the decay ratios ($k_c \rightarrow t/k_t \rightarrow c$) for 2 and 3 included in an OA

capsule were calculated to be 1.6 and 13.3, respectively. Clearly, the *trans* isomer is much more favored when the 4- substitution in the aryl group is CH₃.

Finally, to check the recyclability of the photochromic process, we prepared the *cis* isomer by UV irradiation and attempted to reverse it to the *trans* by visible light irradiation. As seen in Figures 14 and 15, the isomerization process within an OA capsule is reversible. Selective UV irradiation leads to enhancement of *cis* while selective visible irradiation reverses it to the *trans*. The fact that the isomer composition does not change between cycles suggests that the torsional motion of the phenyl group is tolerated by the capsule, and after each N=N rotation, the capsule with its content returns to its original structure. This suggests that arylazoisoxazoles can serve as reversible photoswitches even in a confined environment. Furthermore, the use of an OA capsule allows the use of these systems as photoswitches in aqueous medium. Results reported here, although confined to arylazoisoxazoles, are also applicable to other azoheteroarenes. We plan to pursue the steady-state and ultrafast time-resolved experiments on isomerization of other OA encapsulated azoheteroarenes in the future.

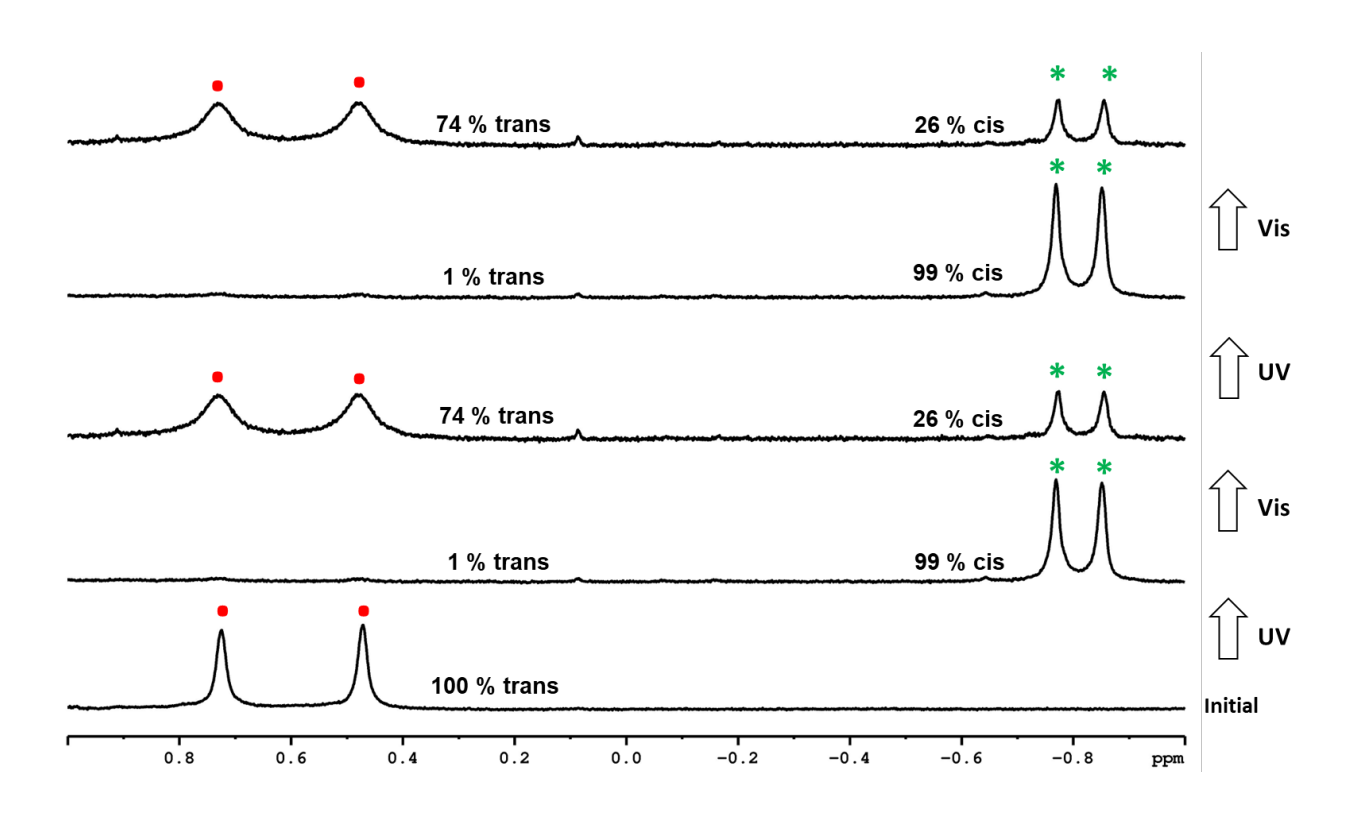


Figure 14: Partial ¹H-NMR spectra monitoring the photoisomerization of trans-2@OA₂ ([OA] = 1 mM, [trans-2] = 0.5 mM). NMR recorded after alternate UV (350 \pm 20 nm) and visible (420 \pm 20 nm) light irradiations. Each irradiation is for 30 minutes. Red dots denote the methyl signals of trans-2 and green asterisks denote the methyl signals of cis-2.

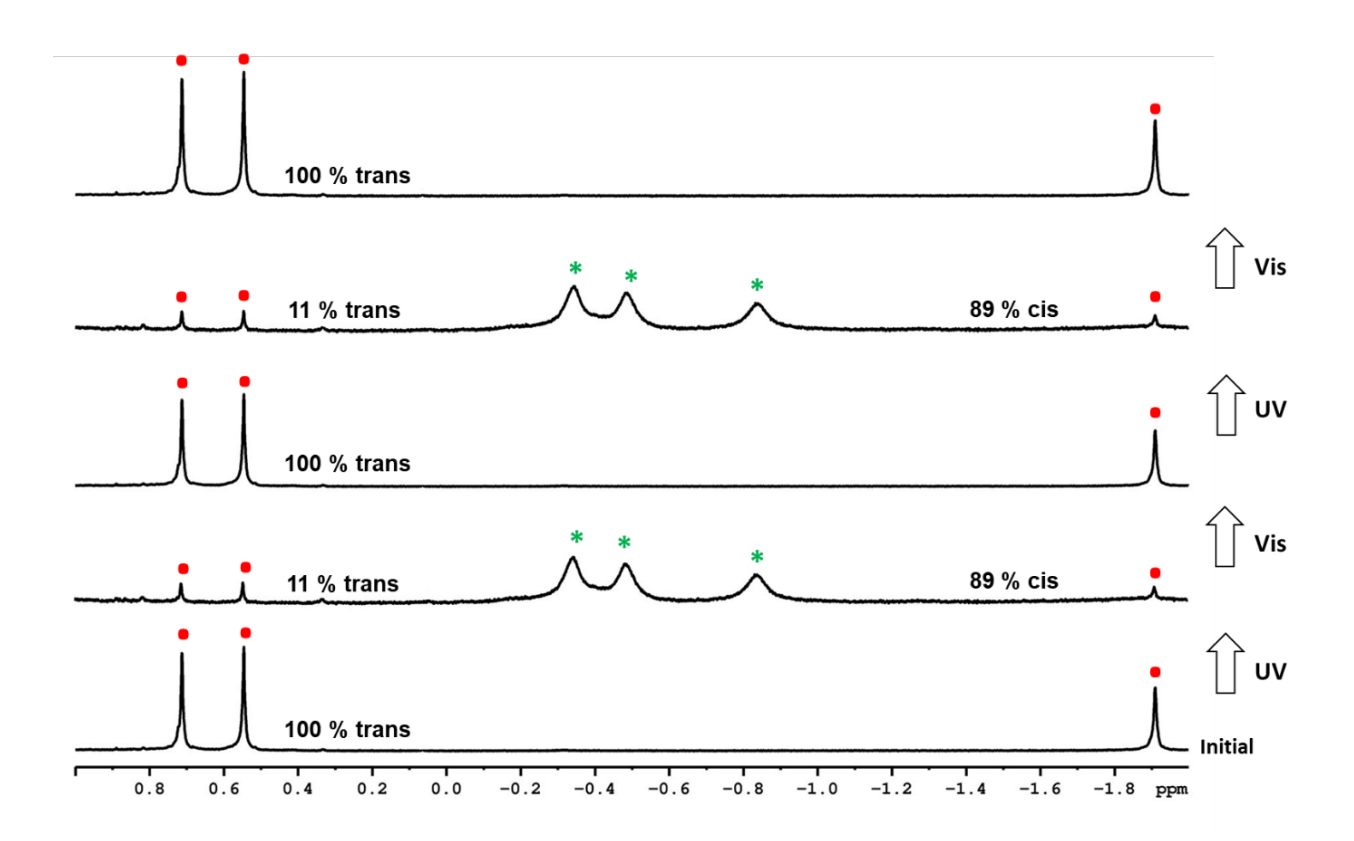


Figure 15: Partial ¹H-NMR spectra monitoring the photoisomerization of trans-3@OA₂ ([OA] = 1 mM, [trans-3] = 0.5 mM). NMR recorded after alternate UV (350 \pm 20 nm) and visible (420 \pm 20 nm) light irradiations. Each irradiation is for 30 minutes. Red dots denote the methyl signals of trans-3 and green asterisks denote the methyl signals of cis-3.

Conclusions

Azobenzenes have attracted considerable attention as photochromic switches because of their well separated S₁ and S₂ absorptions and relatively poor thermal stability of the *cis*-isomer. In addition, because the nitrogen can undergo inversion, geometrical isomerization can occur through more pathways besides torsional rotation that is only available for stilbenes. The well-separated S₁ and S₂ states provide opportunities for reactions from lower and upper excited states. These unusual features have attracted the attention of photochemists, ultrafast spectroscopists, and theoretical chemists focused on fundamental understanding of the excited state dynamics of azobenzenes and stilbenes. The photochromic properties of azobenzene continue to attract chemists interested in their applications in biology, materials science, medicinal chemistry and chemistry in general.

During the last decade of investigations on controlling the thermal stability of the cis isomer and to enhancing the rates of switching between isomers, azoheteroarenes, where one of the phenyl rings is replaced by heterocyclic ring, were examined. In this study, we have examined the photochemistry of select arylazoisoxazoles included within a confined reaction vessel. Our interest was to probe how one could control the chemistry of molecules by restricting their freedom through spatial confinement. In this context, we have used a synthetic organic capsule as the reaction vessel. Keeping in mind that structure, dynamics and reactivity are interrelated, we have characterized the structure of the host-guest complexes by ¹H NMR, studied the dynamics through variable temperature NMR, and thermal and photochemical isomerization by following its progress through ¹H NMR. We have established that the guest molecules trapped within an OA capsule have restricted mobility. Depending on the molecular size, the guest molecule is able to tumble (flip) within the OA capsule with the capsule either fully closed or partially opened. This observation suggests that molecules, upon activation, would be able to undergo reactions. We have established with the help of two arylazoisoxazoles that the weak C–H--- π interaction between the host and guest plays a role in the excited state dynamics of these molecules. In addition, photoisomerization was found to be reversible with the capsule closed at all times. This provides an opportunity to examine photoswitching properties of arylazoisoxazoles, and of azoheteroarenes in general, captured in a closed container in water. Further, the difference in binding of photoisomers in the encapsulated medium dictated by the substituents and the

solubilization of guest in water open up the possibility for delivery of drug molecules in photopharmacological applications. We are aware that the mechanistic conclusions drawn here are based on qualitative reasoning. The system and the preliminary results favor undertaking in-depth ultrafast time resolved experimental and high-level computational studies. We plan to pursue these in the future.

Orcid numbers

Amal Sam Sunny	0000-0003-3440-3636
Vaidhyanathan Ramamurthy	0000-0002-3168-2185
Pravesh Kumar	0000-0002-8648-6739
Sugumar Venkataramani	0000-0002-6465-3655
Elliott C. Cleven	0009-0003-4113-2894
Jamie D. Walls	0000-0003-4813-852X

Conflicts of interest

There are no conflicts to declare.

Supporting information

Electronic Supplementary Information (ESI) available. 1D and 2 D NMR spectra of host-guest complexes, progress of reaction within capsule as followed by ¹H NMR, MD simulated structures of host-guest complexes, NMR spectra related to competitive binding, Eyring and Arrhenius plots, ¹H NMR spectra and data related to thermal and photochemical isomerizations.

Acknowledgements

VR thanks the generous support of NSF for support of this research (CHE-2204046). SV thanks the Science and Engineering Research Board (SERB), New Delhi for the financial support (CRG/2023/003861). EC and JW acknowledge support from the NSF (CHE-1807724). VR and AS thank Prof. Rajeev Prabhakar and Mr. Sreerag M. Narayanan for valuable help with MD simulations.

References

- 1. Hammond, G. S., Restructuring of Chemistry and Chemical Curricula. *Pure Appl. Chem.* **1970**, *22*, 3-16.
- 2. Cram, D. J.; Hammond, G. S., Organic Chemistry; McGraw-Hill: New York, US, 1959.
- 3. Ramamurthy, V., Photochemistry within a Water-Soluble Organic Capsule. *Acc. Chem. Res.* **2015**, *48*, 2904-2917.
- 4. Ramamurthy, V., Photochemistry in a Capsule: Controlling Excited State Dynamics Via Confinement. *Chem. Commun. (Cambridge, U. K.)* **2022**, *58*, 6571-6585.
- 5. Ramamurthy, V.; Sen, P.; Elles, C. G., Ultrafast Excited State Dynamics of Spatially Confined Organic Molecules. *J. Phys. Chem. A* **2022**, *126*, 4681-4699.
- 6. Ramamurthy, V., *Photochemistry in Organized and Constrained Media*. VCH: New York, 1991.
- 7. Ramamurthy, V.; Inoue, Y., *Supramolecular Photochemistry*. John Wiley: Hoboken, 2011.
- 8. Gibb, C. L. D.; Gibb, B. C., Well-Defined, Organic Nanoenvironments in Water: The Hydrophobic Effect Drives a Capsular Assembly. *J. Am. Chem. Soc.* **2004**, *126*, 11408-11409.
- Jayaraj, N.; Zhao, Y.; Parthasarathy, A.; Porel, M.; Liu, R. S. H.; Ramamurthy, V., Nature of Supramolecular Complexes Controlled by the Structure of the Guest Molecules: Formation of Octa Acid Based Capsuleplex and Cavitandplex. *Langmuir* 2009, 25, 10575-10586.
- Kumar, P.; Srivastava, A.; Sah, C.; Devi, S.; Venkataramani, S., Arylazo-3,5-Dimethylisoxazoles: Azoheteroarene Photoswitches Exhibiting High Z-Isomer Stability, Solid-State Photochromism, and Reversible Light-Induced Phase Transition. *Chem. - Eur. J.* 2019, 25, 11924-11932.

- 11. Otolski, C. J.; Mohan Raj, A.; Ramamurthy, V.; Elles, C. G., Ultrafast Dynamics of Encapsulated Molecules Reveals New Insight on the Photoisomerization Mechanism for Azobenzenes. *J. Phys. Chem. Lett.* **2019**, *10*, 121-127.
- 12. Otolski, C. J.; Raj, A. M.; Ramamurthy, V.; Elles, C. G., Spatial Confinement Alters the Ultrafast Photoisomerization Dynamics of Azobenzenes. *Chem. Sci.* **2020**, *11*, 9513-9523.
- Mohan Raj, A.; Ramamurthy, V., Volume Conserving Geometric Isomerization of Encapsulated Azobenzenes in Ground and Excited States and as Radical Ion. *Org. Lett.* 2017, 19, 6116-6119.
- 14. Gunther, H., Nmr Spectroscopy; John Wiley: Chichester, 1992.
- 15. Weiss, R. G.; Ramamurthy, V.; Hammond, G. S., Photochemistry in Organized and Confining Media: A Model. *Acc. Chem. Res.* **1993**, *26*, 530-536.
- Ramamurthy, V.; Weiss, R. G.; Hammond, G. S., A Model for the Influence of Organized Media on Photochemical Reactions. In *Advances in Photochemistry*, Volman, D. H.; Hammond, G. S.; Neckers, D. C., Eds. John Wiley & Sons: New York, 1993; Vol. 18, pp 67-236.
- 17. Baldridge, A.; Samanta, S. R.; Jayaraj, N.; Ramamurthy, V.; Tolbert, L. M., Activation of Fluorescent Protein Chromophores by Encapsulation. *J. Am. Chem. Soc.* **2010**, *132*, 1498-1499.
- 18. Baldridge, A.; Samanta, S. R.; Jayaraj, N.; Ramamurthy, V.; Tolbert, L. M., Steric and Electronic Effects in Capsule-Confined Green Fluorescent Protein Chromophores. *J. Am. Chem. Soc.* **2011**, *133*, 712-715.
- 19. Kulasekharan, R.; Choudhury, R.; Prabhakar, R.; Ramamurthy, V., Restricted Rotation Due to the Lack of Free Space within a Capsule Translates into Product Selectivity: Photochemistry of Cyclohexyl Phenyl Ketones within a Water-Soluble Organic Capsule. *Chem. Commun. (Cambridge, U. K.)* **2011**, *47*, 2841-2843.
- 20. Kawahara, S.-I.; Tsuzuki, S.; Uchimaru, T., Theoretical Study of the C-F/Π Interaction: Attractive Interaction between Fluorinated Alkane and an Electron-Deficient Π-System. *J. Phys. Chem. A* **2004**, *108*, 6744-6749.

- 21. Parthasarathy, A.; Kaanumalle, L. S.; Ramamurthy, V., Controlling Photochemical Geometric Isomerization of a Stilbene and Dimerization of a Styrene Using a Confined Reaction Cavity in Water. *Org. Lett.* **2007**, *9*, 5059-5062.
- 22. Parthasarathy, A.; Ramamurthy, V., Role of Free Space and Weak Interactions on Geometric Isomerization of Stilbenes Held in a Molecular Container. *Photochem. Photobiol. Sci.* **2011**, *10*, 1455-1462.
- 23. Otolski, C. J.; Mohan Raj, A.; Sharma, G.; Prabhakar, R.; Ramamurthy, V.; Elles, C. G., Ultrafast Trans → Cis Photoisomerization Dynamics of Alkyl-Substituted Stilbenes in a Supramolecular Capsule. *J. Phys. Chem. A* **2019**, *123*, 5061-5071.
- 24. Raj, A. M.; Sharma, G.; Prabhakar, R.; Ramamurthy, V., Space Constrained Stereoselective Geometric Isomerization of 1,2-Diphenylcyclopropane and Stilbenes in an Aqueous Medium. *Org. Lett.* **2019**, *21*, 5243-5247.
- Calbo, J.; Weston, C. E.; White, A. J. P.; Rzepa, H. S.; Contreras-Garcia, J.; Fuchter, M. J., Tuning Azoheteroarene Photoswitch Performance through Heteroaryl Design. *J. Am. Chem. Soc.* 2017, *139*, 1261-1274.
- Devi, S.; Saraswat, M.; Grewal, S.; Venkataramani, S., Evaluation of Substituent Effect in Z-Isomer Stability of Arylazo-1h-3,5-Dimethylpyrazoles: Interplay of Steric, Electronic Effects and Hydrogen Bonding. *J. Org. Chem.* 2018, 83, 4307-4322.
- 27. Wang, Y.-T.; Liu, X.-Y.; Cui, G.; Fang, W.-H.; Thiel, W., Photoisomerization of Arylazopyrazole Photoswitches: Stereospecific Excited-State Relaxation. *Angew. Chem., Int. Ed.* **2016**, *55*, 14009-14013.
- 28. Weingart, O.; Lan, Z.; Koslowski, A.; Thiel, W., Chiral Pathways and Periodic Decay in Cis-Azobenzene Photodynamics. *J. Phys. Chem. Lett.* **2011**, *2*, 1506-1509.
- 29. Boeckmann, M.; Doltsinis, N. L.; Marx, D., Unraveling a Chemically Enhanced Photoswitch: Bridged Azobenzene. *Angew. Chem., Int. Ed.* **2010**, *49*, 3382-3384.
- 30. Slavov, C.; Yang, C.; Heindl, A. H.; Wegner, H. A.; Dreuw, A.; Wachtveitl, J., Thiophenylazobenzene: An Alternative Photoisomerization Controlled by Lone-Pair···Π Interaction. *Angew. Chem., Int. Ed.* **2020**, *59*, 380-387.

- 31. Simeth, N. A.; Crespi, S.; Fagnoni, M.; Konig, B., Tuning the Thermal Isomerization of Phenylazoindole Photoswitches from Days to Nanoseconds. *J. Am. Chem. Soc.* **2018**, *140*, 2940-2946.
- 32. Nenov, A., et al., Uv-Light-Induced Vibrational Coherences: The Key to Understand Kasha Rule Violation in Trans-Azobenzene. *J. Phys. Chem. Lett.* **2018**, *9*, 1534-1541.
- 33. Mukherjee, A.; Seyfried, M. D.; Ravoo, B. J., Azoheteroarene and Diazocine Molecular Photoswitches: Self-Assembly, Responsive Materials and Photopharmacology. *Angew. Chem., Int. Ed.* **2023**, *62*, e202304437.
- 34. Kumar, P.; Gupta, D.; Grewal, S.; Srivastava, A.; Kumar Gaur, A.; Venkataramani, S., Multiple Azoarenes Based Systems Photoswitching, Supramolecular Chemistry and Application Prospects. *Chem. Rec.* **2022**, *22*, e202200074.
- 35. Hoeglsperger, F.; Larik, F. A.; Bai, C.; Seyfried, M. D.; Daniliuc, C.; Klaasen, H.; Thordarson, P.; Beves, J. E.; Ravoo, B. J., Water-Soluble Arylazoisoxazole Photoswitches. *Chem. Eur. J.* **2023**, *29*, e202302069.
- 36. Dolai, A.; Bhunia, S.; Manna, K.; Bera, S.; Box, S. M.; Bhattacharya, K.; Saha, R.; Sarkar, S.; Samanta, S., Visible-Light-Sensitive Photoliquefiable Arylazoisoxazoles for the Solar Energy Conversion, Storage and Controlled-Release of Heat at Room Temperature or Lower Temperatures. *ChemSusChem* **2024**, e202301700.
- Stricker, L.; Boeckmann, M.; Kirse, T. M.; Doltsinis, N. L.; Ravoo, B. J.,
 Arylazopyrazole Photoswitches in Aqueous Solution: Substituent Effects,
 Photophysical Properties, and Host-Guest Chemistry. *Chem. Eur. J.* 2018, 24, 8639-8647.
- 38. Kortekaas, L.; Simke, J.; Kurka, D. W.; Ravoo, B. J., Rapid Photoswitching of Low Molecular Weight Arylazoisoxazole Adhesives. *ACS Appl. Mater. Interfaces* **2020**, *12*, 32054-32060.
- 39. Kortekaas, L.; Simke, J.; Arndt, N. B.; Boeckmann, M.; Doltsinis, N. L.; Ravoo, B. J., Acid-Catalysed Liquid-to-Solid Transitioning of Arylazoisoxazole Photoswitches. *Chem. Sci.* **2021**, *12*, 11338-11346.

- Rossi, R.; Salvini, A.; Pizzo, B.; Frediani, M.; Wiersma, D. S.; Parmeggiani, C.;
 Martella, D., Photoresponsive Adhesives Based on Arylazoisoxazoles-Containing
 Polymers. *Macromol. Mater. Eng.* 2023, 308, 2200504.
- 41. Meteling, H. J.; Bosse, F.; Schlichter, L.; Tyler, B. J.; Arlinghaus, H. F.; Ravoo, B. J., Versatile Surface Patterning with Low Molecular Weight Photoswitches. *Small* **2022**, *18*, 2203245.
- 42. Crespi, S.; Simeth, N. A.; König, B., Heteroaryl Azo Dyes as Molecular Photoswitches. *Nat. Rev. Chem.* **2019**, *3*, 133-146.
- 43. Surbhi, G.; Gupta, D.; Gaur, A. K.; Saraswat, M.; Sugumar, V., Azoheteroarene Photoswitches Synthesis, Photoswitching and Utility. In *Photoisomerization: Causes, Behavior and Effects*, Sampedro, D., Ed. Nova Publishers: USA, 2019.
- 44. Kortekaas, L.; Simke, J.; Kurka, D. W.; Ravoo, B. J., Rapid Photoswitching of Low Molecular Weight Arylazoisoxazole Adhesives. *ACS Appl. Mater. Interfaces* **2020**, *12*, 32054–32060.
- 45. Gerkman, M. A.; Gibson, R. S. L.; Calbo, J.; Shi, Y.; Fuchter, J.; Han, G. G. D., Arylazopyrazoles for Long-Term Thermal Energy Storage and Optically Triggered Heat Release Below 0 °C. *J. Am. Chem. Soc.* **2020**, *142*, 8688–8695.
- 46. Stricker, L.; Fritz, E. C.; Peterlechner, M.; Doltsinis, N. L.; Ravoo, B. J., Arylazopyrazoles as Light-Responsive Molecular Switches in Cyclodextrin-Based Supramolecular Systems. *J. Am. Chem. Soc.* **2016**, *138*, 4547–4554.
- Hoffman, R. E.; Becker, E. D., Temperature Dependence of the 1h Chemical Shift of Tetramethylsilane in Chloroform, Methanol, and Dimethylsulfoxide. *J. Magn. Reson.* 2005, 176, 87-98.
- 48. *Curve Fitting Toolbox : For Use with Matlab*® : *User'S Guide*; Version 1. Natick, MA : MathWorks, 2001., 2001.
- 49. Lente, G.; Fabian, I.; Poe, A. J., A Common Misconception About the Eyring Equation. *New J. Chem.* **2005**, *29*, 759-760.

- 50. Becke, A. D., Density-Functional Exchange-Energy Approximation with Correct Asymptotic Behavior. *Phys. Rev. A: Gen. Phys.* **1988**, *38*, 3098-3100.
- 51. Becke, A. D., Density-Functional Thermochemistry. Iii. The Role of Exact Exchange. *J. Chem. Phys.* **1993**, *98*, 5648-5652.
- 52. Grimme, S.; Ehrlich, S.; Goerigk, L., Effect of the Damping Function in Dispersion Corrected Density Functional Theory. *J. Comput. Chem.* **2011**, *32*, 1456-1465.
- 53. Frisch, M.; Trucks, G.; Schlegel, H.; Scuseria, G.; Robb, M.; Cheeseman, J.; Scalmani, G.; Barone, V.; Mennucci, B.; Petersson, G., D.01; Gaussian, Inc.: Wallingford, Ct. *Gaussian 09* **2009**.
- 54. Francl, M. M.; Pietro, W. J.; Hehre, W. J.; Binkley, J. S.; Gordon, M. S.; DeFrees, D. J.; Pople, J. A., Self-Consistent Molecular Orbital Methods. Xxiii. A Polarization-Type Basis Set for Second-Row Elements. *J. Chem. Phys.* 1982, 77, 3654-3665.
- 55. Rassolov, V. A.; Ratner, M. A.; Pople, J. A.; Redfern, P. C.; Curtiss, L. A., 6-31g* Basis Set for Third-Row Atoms. *J. Comput. Chem.* **2001**, *22*, 976-984.
- 56. Wang, J.; Wang, W.; Kollman, P. A.; Case, D. A., Automatic Atom Type and Bond Type Perception in Molecular Mechanical Calculations. *J. Mol. Graphics Modell.* **2006**, *25*, 247-260.
- 57. Trott, O.; Olson, A. J., Autodock Vina: Improving the Speed and Accuracy of Docking with a New Scoring Function, Efficient Optimization, and Multithreading. *J. Comput. Chem.* **2010**, *31*, 455-461.
- 58. Hess, B. In *Gromacs 4: Algorithms for Highly Efficient, Load-Balanced, and Scalable Molecular Simulation*, American Chemical Society: 2009; p COMP.
- 59. Pronk, S., et al., Gromacs 4.5: A High-Throughput and Highly Parallel Open Source Molecular Simulation Toolkit. *Bioinformatics* **2013**, *29*, 845-854.
- 60. Case, D. A.; Cheatham Iii, T. E.; Darden, T.; Gohlke, H.; Luo, R.; Merz Jr, K. M.; Onufriev, A.; Simmerling, C.; Wang, B.; Woods, R. J., The Amber Biomolecular Simulation Programs. *Journal of Computational Chemistry* **2005**, *26*, 1668-1688.

- 61. Price, D. J.; Brooks, C. L., III, A Modified Tip3p Water Potential for Simulation with Ewald Summation. *J. Chem. Phys.* **2004**, *121*, 10096-10103.
- 62. Hess, B.; Bekker, H.; Berendsen, H. J. C.; Fraaije, J. G. E. M., Lincs: A Linear Constraint Solver for Molecular Simulations. *J. Comput. Chem.* **1997**, *18*, 1463-1472.
- 63. Miyamoto, S.; Kollman, P. A., Settle: An Analytical Version of the Shake and Rattle Algorithm for Rigid Water Models. *J. Comput. Chem.* **1992**, *13*, 952-962.
- 64. Darden, T.; York, D.; Pedersen, L., Particle Mesh Ewald: An N·Log(N) Method for Ewald Sums in Large Systems. *The Journal of Chemical Physics* **1993**, *98*, 10089-10092.
- 65. Kumari, R.; Kumar, R.; Lynn, A., G_Mmpbsa-a Gromacs Tool for High-Throughput Mm-Pbsa Calculations. *J. Chem. Inf. Model.* **2014**, *54*, 1951-1962.
- 66. Krieger, E.; Vriend, G., Models@Home: Distributed Computing in Bioinformatics Using a Screensaver Based Approach. *Bioinformatics* **2002**, *18*, 315-318.
- 67. Pettersen, E. F.; Goddard, T. D.; Huang, C. C.; Couch, G. S.; Greenblatt, D. M.; Meng, E. C.; Ferrin, T. E., Ucsf Chimera-a Visualization System for Exploratory Research and Analysis. *J. Comput. Chem.* **2004**, *25*, 1605-1612.
- 68. Humphrey, W.; Dalke, A.; Schulten, K., Vmd: Visual Molecular Dynamics. *Journal of Molecular Graphics* **1996**, *14*, 33-38.
- 69. Kulasekharan, R.; Jayaraj, N.; Porel, M.; Choudhury, R.; Sundaresan, A. K.; Parthasarathy, A.; Ottaviani, M. F.; Jockusch, S.; Turro, N. J.; Ramamurthy, V., Guest Rotations within a Capsuleplex Probed by Nmr and Epr Techniques. *Langmuir* **2010**, *26*, 6943-6953.
- 70. Choudhury, R.; Barman, A.; Prabhakar, R.; Ramamurthy, V., Hydrocarbons Depending on the Chain Length and Head Group Adopt Different Conformations within a Water-Soluble Nanocapsule: 1h Nmr and Molecular Dynamics Studies. *J. Phys. Chem. B* **2013**, *117*, 398-407.

- 71. Porel, M.; Jayaraj, N.; Kaanumalle, L. S.; Maddipatla, M. V. S. N.; Parthasarathy, A.; Ramamurthy, V., Cavitand Octa Acid Forms a Nonpolar Capsuleplex Dependent on the Molecular Size and Hydrophobicity of the Guest. *Langmuir* **2009**, *25*, 3473-3481.
- 72. Samanta, S. R.; Parthasarathy, A.; Ramamurthy, V., Supramolecular Control During Triplet Sensitized Geometric Isomerization of Stilbenes Encapsulated in a Water Soluble Organic Capsule. *Photochem. Photobiol. Sci.* **2012**, *11*, 1652-1660.
- 73. Ramamurthy, V., Controlling Excited State Chemistry of Organic Molecules in Water through Incarceration. John Wiley & Sons, Inc.: 2021; p 335-369.
- 74. Jayaraj, N.; Jockusch, S.; Kaanumalle, L. S.; Turro, N. J.; Ramamurthy, V., Dynamics of Capsuleplex Formed between Octaacid and Organic Guest Molecules Photophysical Techniques Reveal the Opening and Closing of Capsuleplex. *Can. J. Chem.* 2011, 89, 203-213.
- 75. Samanta, S. R.; Baldridge, A.; Tolbert, L. M.; Ramamurthy, V., Guest/Host Complexes of Octa Acid and Amphiphilic Benzylidene-3-Methylimidazolidinones Exchange Hosts within the Nmr Time Scale. *ACS Omega* **2020**, *5*, 8230-8241.
- 76. Das, A.; Sharma, G.; Kamatham, N.; Prabhakar, R.; Sen, P.; Ramamurthy, V., Ultrafast Solvation Dynamics Reveal That Octa Acid Capsule's Interior Dryness Depends on the Guest. *J. Phys. Chem. A* **2019**, *123*, 5928-5936.
- 77. Besnard, M.; Danten, Y.; Tassaing, T., Dynamics of Solitary Water in Benzene and Hexafluorobenzene: An Infrared and Raman Study. *J. Chem. Phys.* **2000**, *113*, 3741-3748.
- 78. Bandara, H. M. D.; Burdette, S. C., Photoisomerization in Different Classes of Azobenzene. *Chem. Soc. Rev.* **2012**, *41*, 1809-1825.
- 79. Dewar, M. J. S.; Dougherty, R. C., *The Pmo Theory of Organic Chemistry*; Plenum: New York, 1975.
- 80. Rau., H., Azo Compounds. In *Photochromism: Molecules and Systems*, 1 ed.; Dürr, H.; Bouas-Laurent, H., Eds. Elsevier: New York, 1990; pp 165-192.

- 81. Quick, M.; Dobryakov, A. L.; Gerecke, M.; Richter, C.; Berndt, F.; Ioffe, I. N.; Granovsky, A. A.; Mahrwald, R.; Ernsting, N. P.; Kovalenko, S. A., Photoisomerization Dynamics and Pathways of Trans- and Cis-Azobenzene in Solution from Broadband Femtosecond Spectroscopies and Calculations. *J. Phys. Chem. B* **2014**, *118*, 8756-8771.
- 82. Fujino, T.; Tahara, T., Picosecond Time-Resolved Raman Study of Trans-Azobenzene. *J. Phys. Chem. A* **2000**, *104*, 4203-4210.
- 83. Rau, H., Further Evidence for Rotation in the Π,Π^* and Inversion in the N, Π^* Photoisomerization of Azobenzenes. *J. Photochem.* **1984**, *26*, 221-225.
- 84. Rau, H.; Lüddecke, E., On the Rotation-Inversion Controversy on Photoisomerization of Azobenzenes. Experimental Proof of Inversion. *J. Am. Chem. Soc.*, **1982**, *104*, 1616-1620.
- 85. Boeckmann, M.; Doltsinis, N. L.; Marx, D., Nonadiabatic Hybrid Quantum and Molecular Mechanic Simulations of Azobenzene Photoswitching in Bulk Liquid Environment. *J. Phys. Chem. A* **2010**, *114*, 745-754.
- 86. Reichenauer, T.; Boeckmann, M.; Ziegler, K.; Kumar, V.; Ravoo, B. J.; Doltsinis, N. L.; Schluecker, S., Photoswitching of Arylazopyrazoles Upon S1 (Nπ*) Excitation Studied by Transient Absorption Spectroscopy and Ab Initio Molecular Dynamics. *Phys. Chem. Chem. Phys.* 2024, 26, 10832-10840.
- 87. Liu, R. S. H.; Hammond, G. S., The Case of Medium-Dependent Dual Mechanisms for Photoisomerization: One-Bond-Flip and Hula-Twist. *Proc. Natl. Acad. Sci. U. S. A.* **2000**, *97*, 11153-11158.
- 88. Jung, Y. O.; Lee, J. H.; Kim, J.; Schmidt, M.; Moffat, K.; Srajer, V.; Ihee, H., Volume-Conserving Trans-Cis Isomerization Pathways in Photoactive Yellow Protein Visualized by Picosecond X-Ray Crystallography. *Nat. Chem.* **2013**, *5*, 212-220.
- 89. Liu, R. S. H.; Browne, D. T., A Bioorganic View of the Chemistry of Vision: H.T.-N and B.P.-M,N Mechanisms for Reactions of Confined, Anchored Polyenes. *Accounts of Chemical Research* **1986**, *19*, 42-48.

- Fadini, A., et al., Serial Femtosecond Crystallography Reveals That Photoactivation in a Fluorescent Protein Proceeds Via the Hula Twist Mechanism. *J. Am. Chem. Soc.* 2023, 145, 15796-15808.
- 91. Gerwien, A.; Schildhauer, M.; Thumser, S.; Mayer, P.; Dube, H., Direct Evidence for Hula Twist and Single-Bond Rotation Photoproducts. *Nat. Commun.* **2018**, *9*, 1-9.
- 92. Liu, R. S. H.; Asato, A. E., The Primary Process of Vision and the Structure of Bathorhodopsin: A Mechanism for Photoisomerization of Polyenes. *Proc. Natl. Acad. Sci. U. S. A.* **1985**, *82*, 259-263.
- 93. Salvadori, G.; Macaluso, V.; Pellicci, G.; Cupellini, L.; Granucci, G.; Mennucci, B., Protein Control of Photochemistry and Transient Intermediates in Phytochromes. *Nat. Commun.* **2022**, *13*, 6838.
- 94. Fischer, T.; Leitner, J.; Gerwien, A.; Mayer, P.; Dreuw, A.; Dube, H.; Wachtveitl, J., Mechanistic Elucidation of the Hula-Twist Photoreaction in Hemithioindigo. *J. Am. Chem. Soc.* **2023**, *145*, 14811-14822.
- 95. Zimmerman, H. E., Molecular Orbital Correlation Diagrams, Mobius Systems, and Factors Controlling Ground and Excited State Raections. *J. Am. Chem. Soc.* **1966**, *88*, 1566-1567.
- Hammond, G. S., A Correlation of Reaction Rates. *J. Am. Chem. Soc.* 1955, 77, 334–338.
- 97. Boeije, Y.; Olivucci, M., From a One-Mode to a Multi-Mode Understanding of Conical Intersection Mediated Ultrafast Organic Photochemical Reactions. *Chem. Soc. Rev.* **2023**, *52*, 2643-2687.
- 98. Michl, J., Physical Basis of Qualitative Mo Arguments in Organic Photochemistry. *Top. Curr. Chem.* **1974**, *46*, 1-59.
- 99. Michl, J., Historical Introduction. In *Conical Intersections*, Dimcke, W.; Yarkony, D. R.; Koppel, H., Eds. World Scientific: Singapore, 2004; pp ix-xiii.

TOC Graphics

